Review on Mechanical Behavior of High Entropy Alloys

Chair: Prof. Marc A. Meyers
Member: Prof. Shengqiang Cai
Member: Prof. Javier Garay
Member: Prof. Vlado Lubarda
Member: Prof. Vitali Nesterenko

History of HEAs

Developed by Jien-Wei Yeh

Further developed

1980's

2004

1996

Theoretical stand-point

Cantor alloy discovered by Brian Cantor

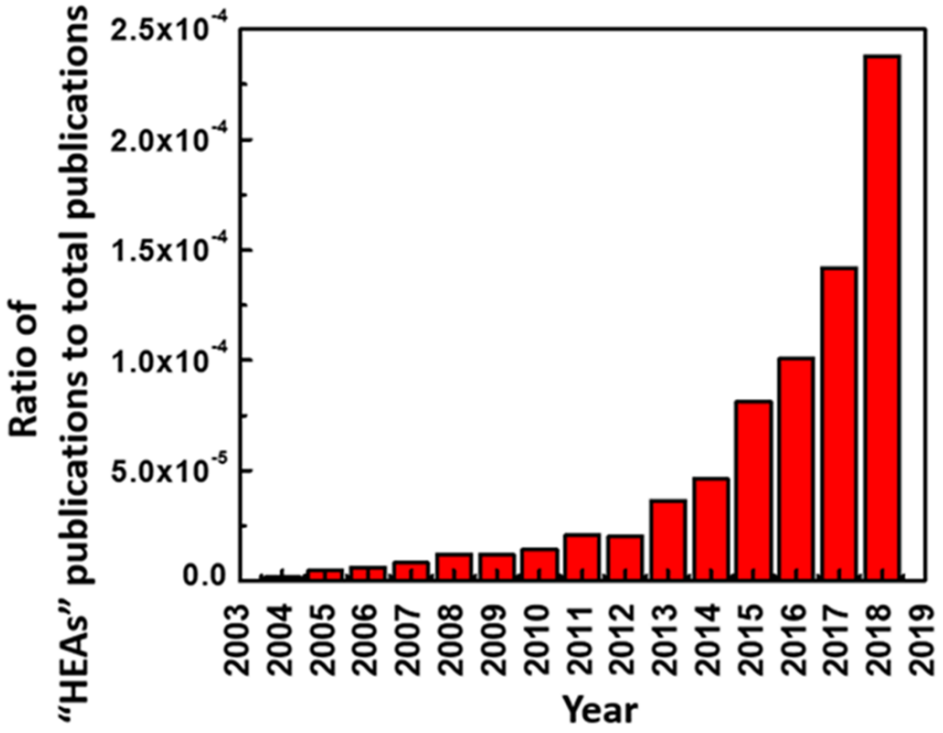

data from the *Web of Science*[2]

Classification of HEAs

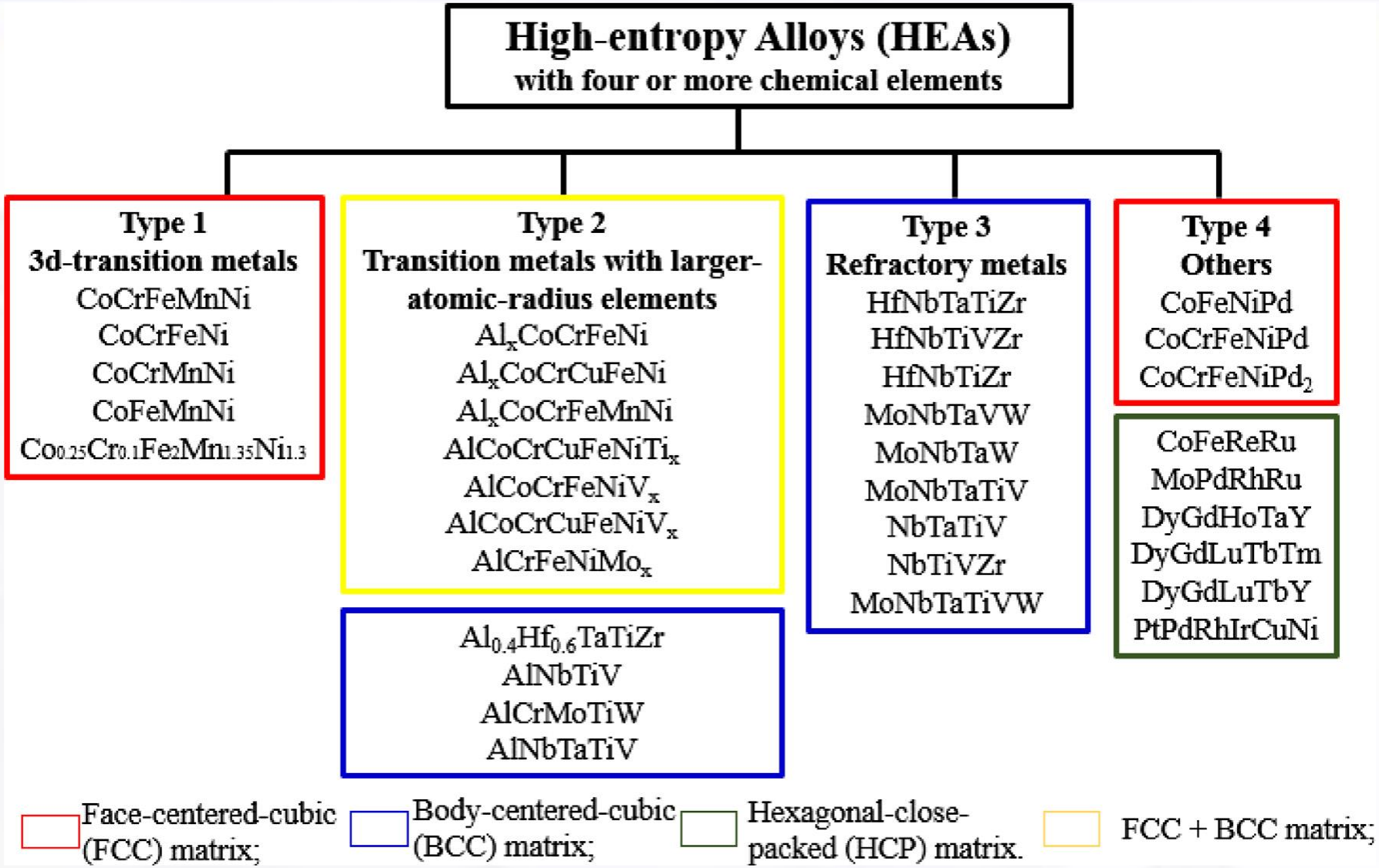

Diao, H. Y., Feng, R., Dahmen, K. A., & Liaw, P. K. (2017). Fundamental deformation behavior in high-entropy alloys: An overview. Current Opinion in Solid State and Materials Science, 21(5), 252-266.

Developed HEA systems

- **Al-Co-Cr-Cu-Fe-Ni alloy system**
- **Derivatives of Al-Co-Cr-Cu-Fe-Ni alloy system:**

  1. Al-Co-Cr-Cu-Ti alloy system

  2. Co-Cr-Fe-Mn-Ni alloy system

  3. Al-Cr-Fe-Mn-Ni alloy system

  …

- **Refractory HEA system:**

  Refractory elements: Cr, Hf, Mo, Nb, Ta, V, W, Zr

Practical Application

High strength

High wearability

Superconducting

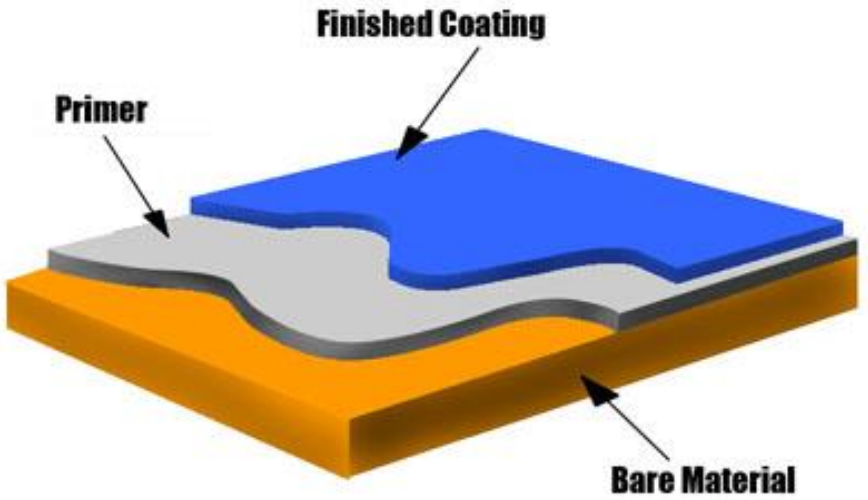

https://www.caeses.com/industries/case-studies/turbine-blade-optimization-including-scallops-for-a-turbocharger/
https://www.globalspec.com/learnmore/materials_chemicals_adhesives/industrial_sealants_coatings/industrial_coatings
https://ricardo.com/news-and-media/news-and-press/ricardo-performance-products-achieves-key-aerospace-manufacturing-certification

Core effects of HEAs

- **1. High entropy effect**
- **2. Sluggish diffusion effect (?)**
- **3. Severe lattice-distortion effect**
- **4. Cocktail effect**
- **5. Short-range ordering**

Tsai, M. H., & Yeh, J. W. (2014). High-entropy alloys: a critical review. Materials Research Letters, 2(3), 107-123.

High entropy effect

$G = H - TS, \Delta S_{config} = RlnN$ (N is number of elements in equimolar ratio)

$$\Delta G_{mix} = \Delta H_{mix} - T\Delta S_{mix} \left(-22 \le \Delta H_{mix} \le \frac{7kJ}{mol}\right) (\Delta S_{mix} > 1.6R)$$

$$S_{config} > 1.6R$$

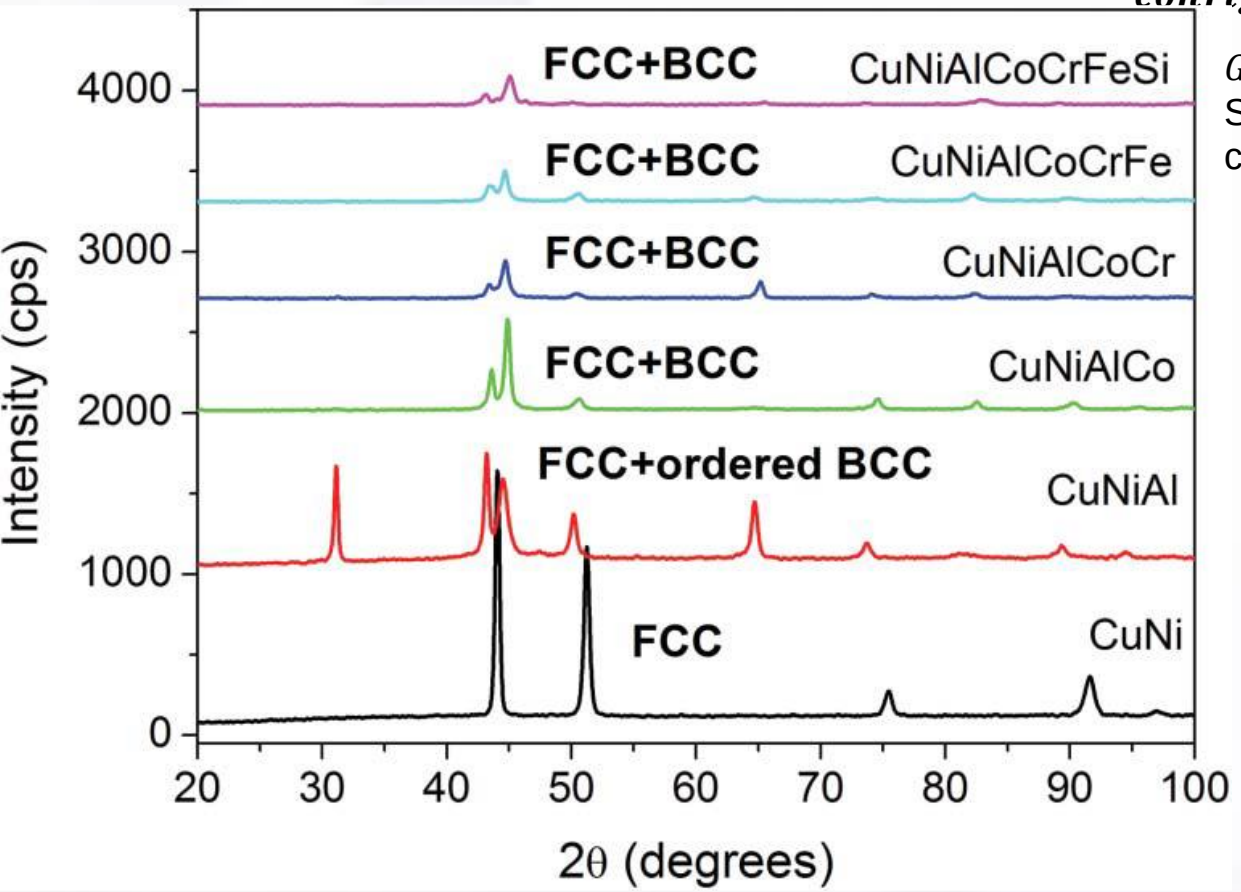

XRD pattern of different multi-component alloy

$G_{SS} < G_{IC}$

Solid solution over intermetallic compounds

$G_{SS} > G_{IC}$

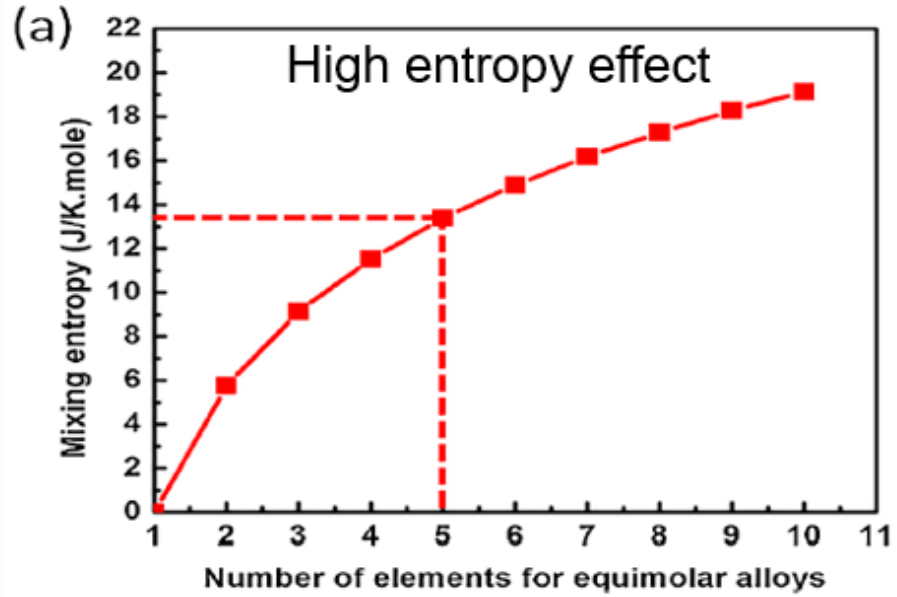

Ming-Hung Tsai & Jien-Wei Yeh (2014) High-Entropy Alloys: A Critical Review, Materials Research Letters, 2:3, 107-123, DOI: 10.1080/21663831.2014.912690

Sluggish diffusion effect

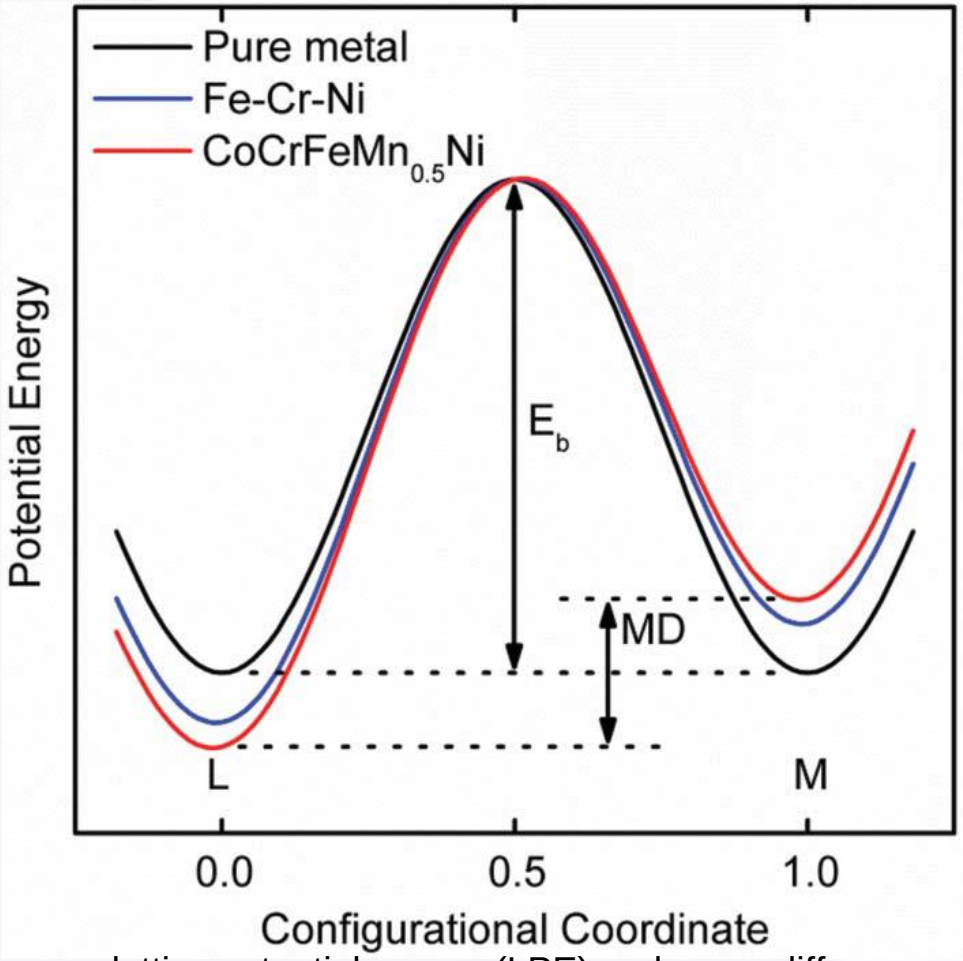

lattice potential energy (LPE) and mean difference when a Ni atom migrates in pure metal

Solute	System	D_0 (10^{-4} m^2/s)	Q (kJ/mol)	$T_m(T_s)$ (K)	Q/T_m	D_{T_m} (10^{-13} m^2/s)
Ni	CoCrFeMnNi	19.7	317.5	1607	0.1975	0.95
	FCC Fe	3	314	1812	0.1733	2.66
	Co	0.43	282.2	1768	0.1596	1.98
	Ni	1.77	285.3	1728	0.1651	4.21
	Fe-15Cr-20Ni	1.5	300	1731	0.1733	1.33
	Fe-15Cr-45Ni	1.8	293	1697	0.1727	1.73
	Fe-22Cr-45Ni	1.1	291	1688	0.1724	1.09
	Fe-15Cr-20Ni-Si	4.8	310	1705	0.1818	1.53

Diffusion parameters for Ni

Higher energy to overcome barrier for atoms to migrate from site L to site M

Ming-Hung Tsai & Jien-Wei Yeh (2014) High-Entropy Alloys: A Critical Review, Materials Research Letters, 2:3, 107-123, DOI: 10.1080/21663831.2014.912690
Tsai KY, Tsai MH, Yeh JW. Sluggish diffusion in Co–Cr–Fe–Mn–Ni high entropy alloys. Acta Mater. 2013;61:4887–4897.

Lattice distortion effect

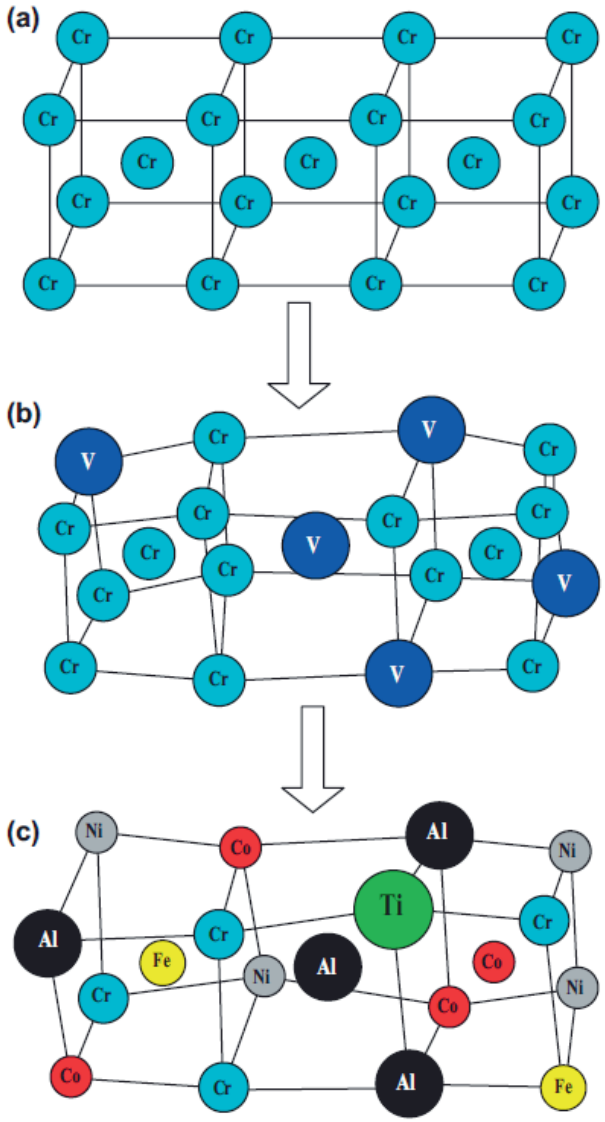

Similar atomic size

Mild distortion effect

Distinct atomic size causes severe lattice distortion effect

Weakened XRD intensity

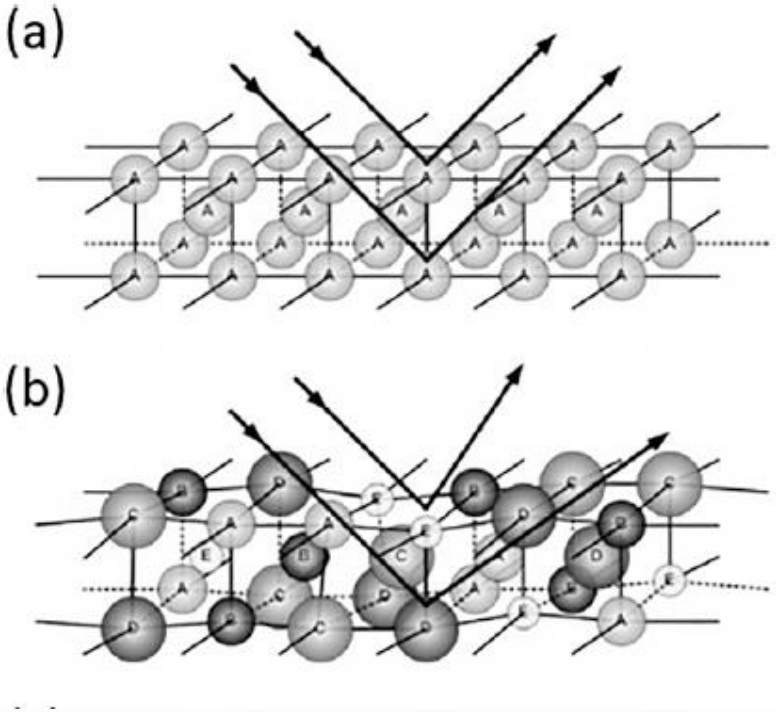

Alvi, S. (2019). Synthesis and Characterization of High Entropy Alloy and Coating (Doctoral dissertation, Luleå tekniska universitet).

Cocktail effect

$Al_xCoCrCuFeNi$ HEA
Change atomic ratio of Al

X=10at%
- 220HV

X=20at%
- 460HV

X=40at%
- 640HV

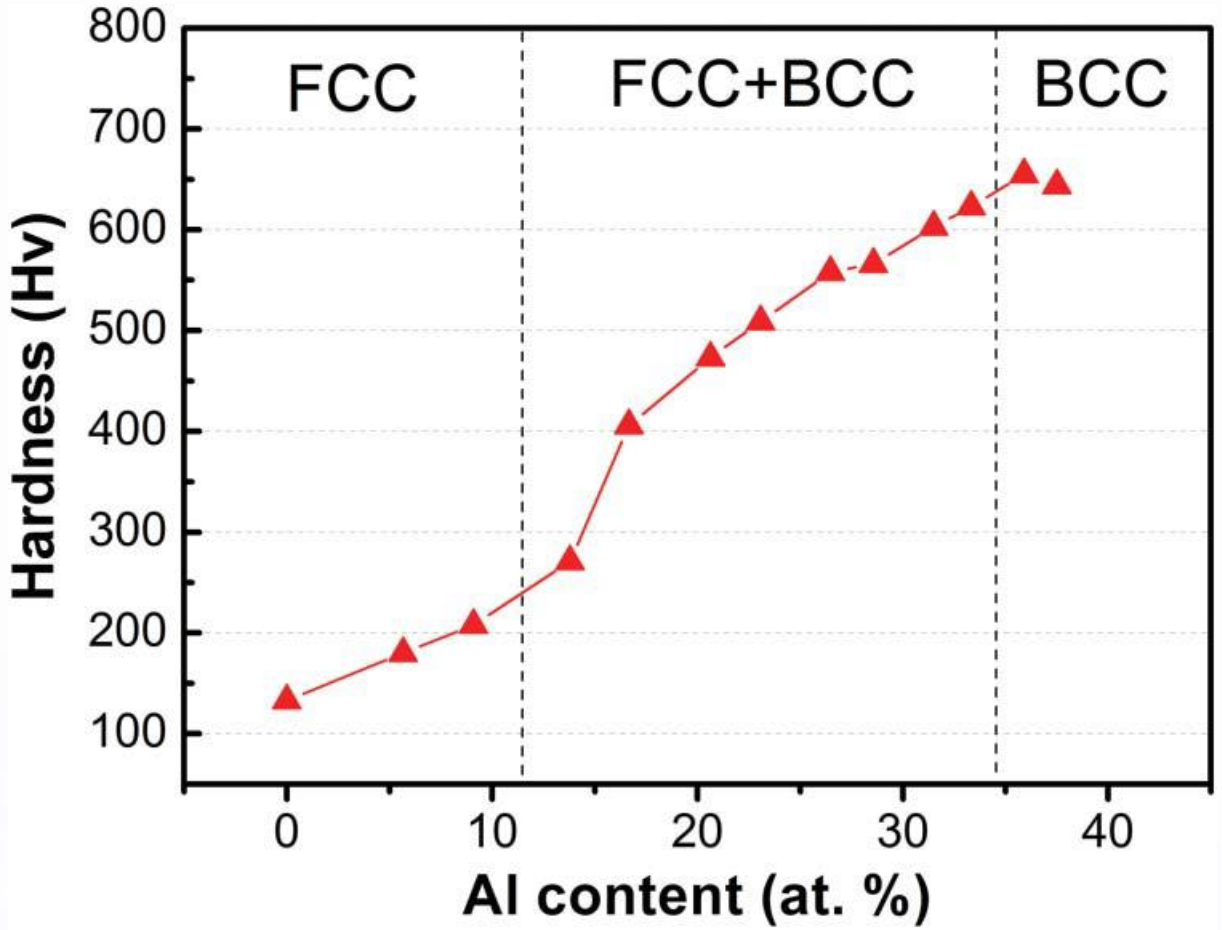

Ming-Hung Tsai & Jien-Wei Yeh (2014) High-Entropy Alloys: A Critical Review, Materials Research Letters, 2:3, 107-123, DOI: 10.1080/21663831.2014.912690

Short-range ordering

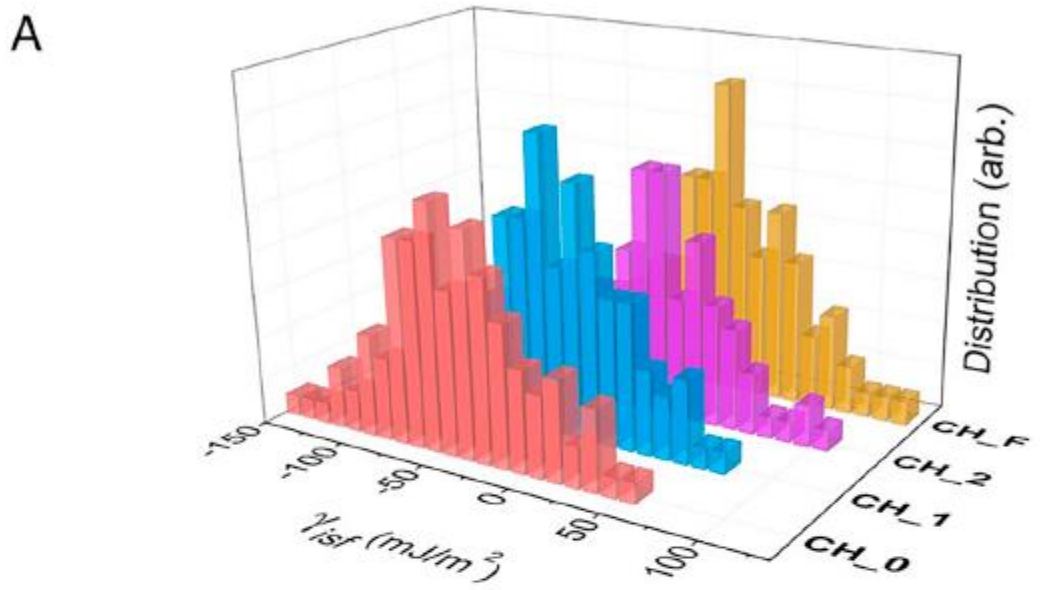

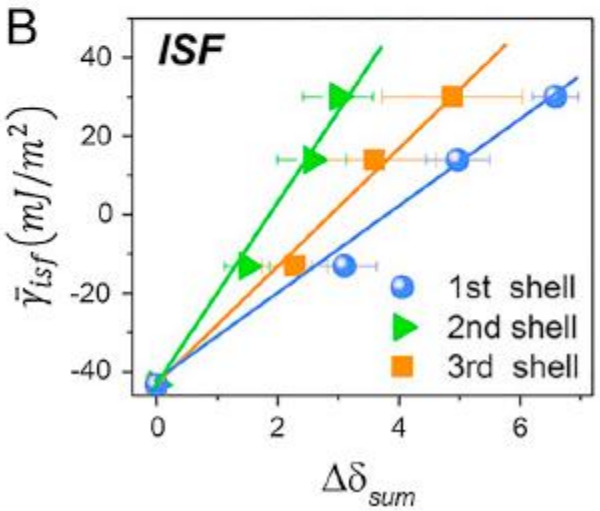

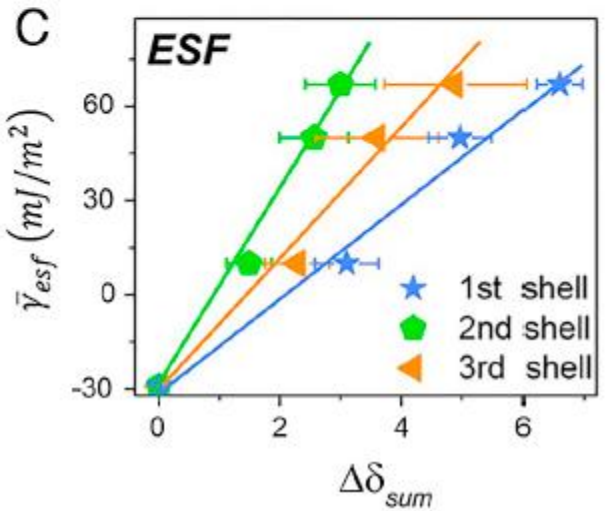

$\bar{\gamma}_{isf}$**(Intrinsic stacking fault energy): -42.9 to 30 mJ/m^2**

$\bar{\gamma}_{esf}$**(Extrinsic stacking fault energy): -27.8 to 66 mJ/m^2**

VEC, lattice distortion, d-electron density

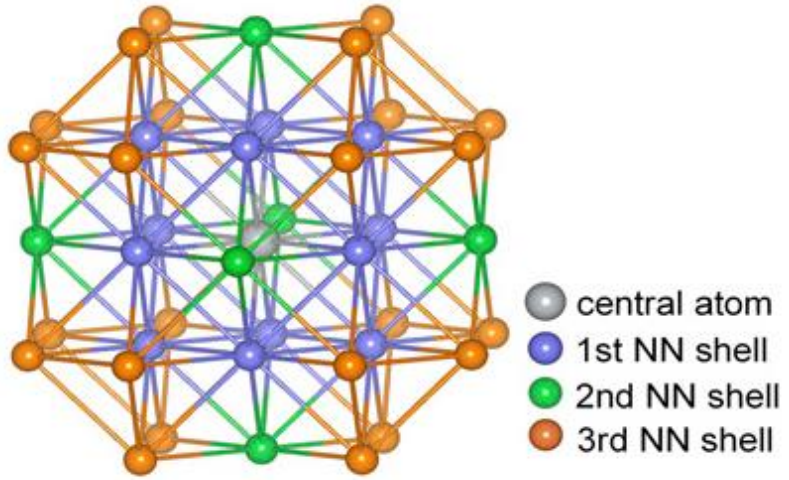

Stacking fault energy and schematic illustration of first three nearest-neighbot shells in FCC

Ding J, Yu Q, Asta M, Ritchie RO. Tunable stacking fault energies by tailoring local chemical order in CrCoNi medium-entropy alloys. Proce Natl Acad Sci 2018;115(36):8919–24.

Hume-Rothery Rule

1. **Mismatch** $= \left(\frac{r_{solute} - r_{solvent}}{r_{solvent}}\right) \times 100 \leq 15\%$
2. **Crystal structure rule**
3. **Valence rule**
4. **Electronegativity rule**

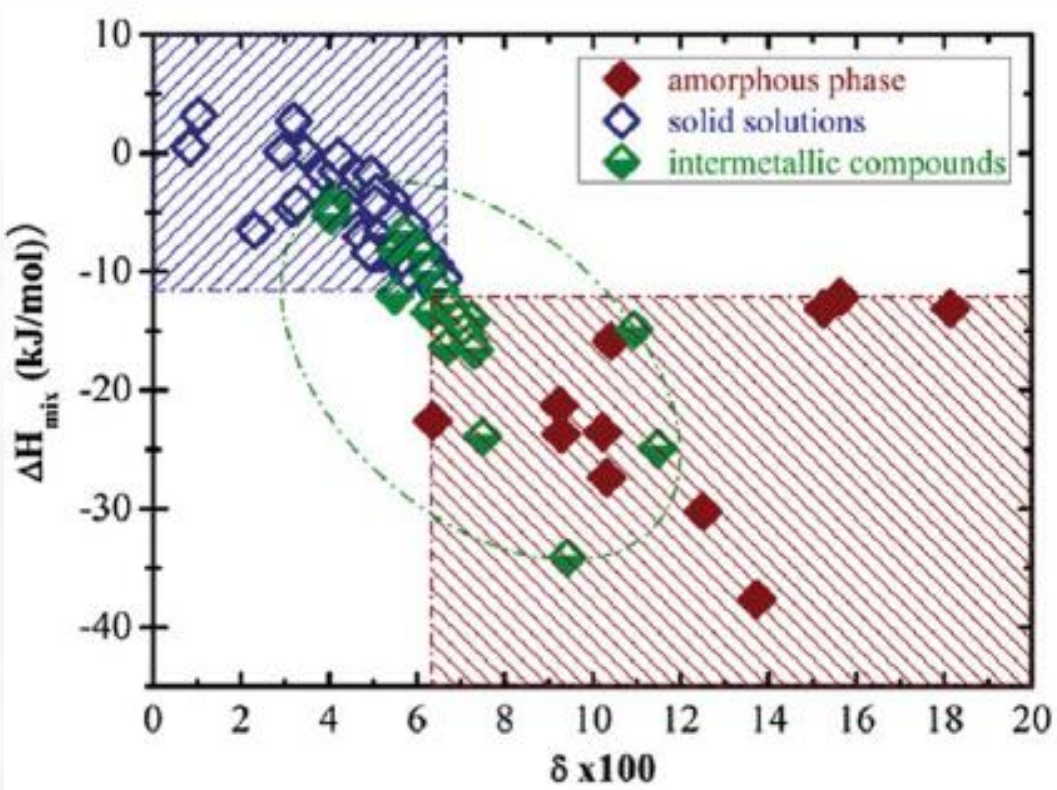

$$\delta = \sqrt{\sum_{i=1}^{N} c_i \left(1 - \frac{r_i}{\bar{r}}\right)^2}$$

$$\bar{r} = \sum_{i=1}^{n} c_i r_i$$

Guo S, Hu Q, Ng C, Liu CT. More than entropy in highentropy alloys: forming solid solutions or amorphous phase. Intermetallics. 2013;41:96–103.

FCC or BCC HEA

(VEC) Valence electron concentration
VEC>8: single FCC
VEC<6.8: single BCC
6.8<VEC<8: co-existence of BCC & FCC

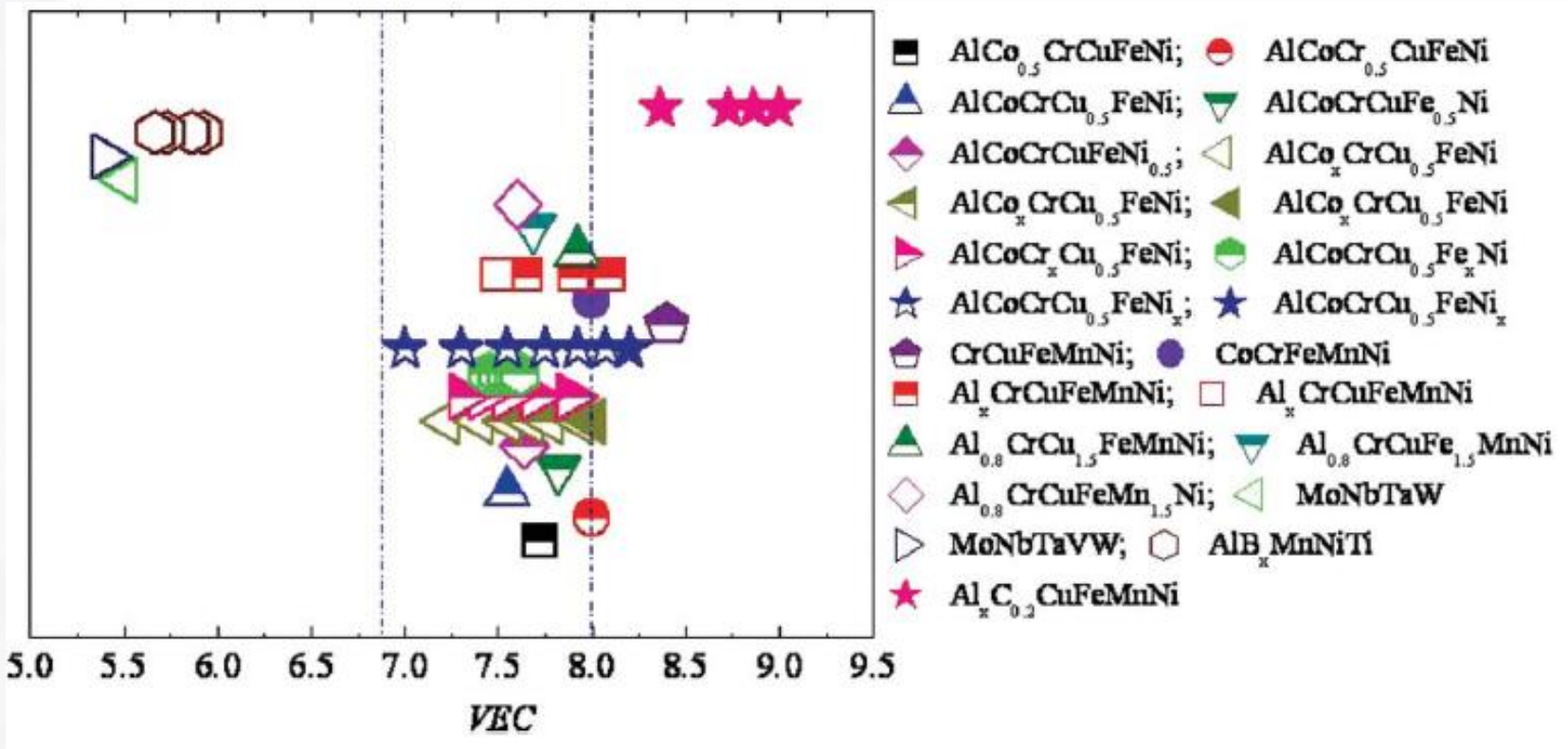

Relationship between VEC and BCC, FCC phase stability

Guo S, Ng C, Lu J, Liu CT. Effect of valence electron concentration on stability of fcc or bcc phase in high entropy alloys. J Appl Phys. 2011;109:103505.

High temperature performance

Resistance to thermal softening: T_T

Softening coefficient of conventional alloy and $AlCoCr_xFeMo_{0.5}Ni$

Alloy	Softening coefficient above T_T
Cr-1.5	−2.32E-4
Cr-2	−1.66E-4
T-800	−3.12E-4
In 718	−3.55E-4

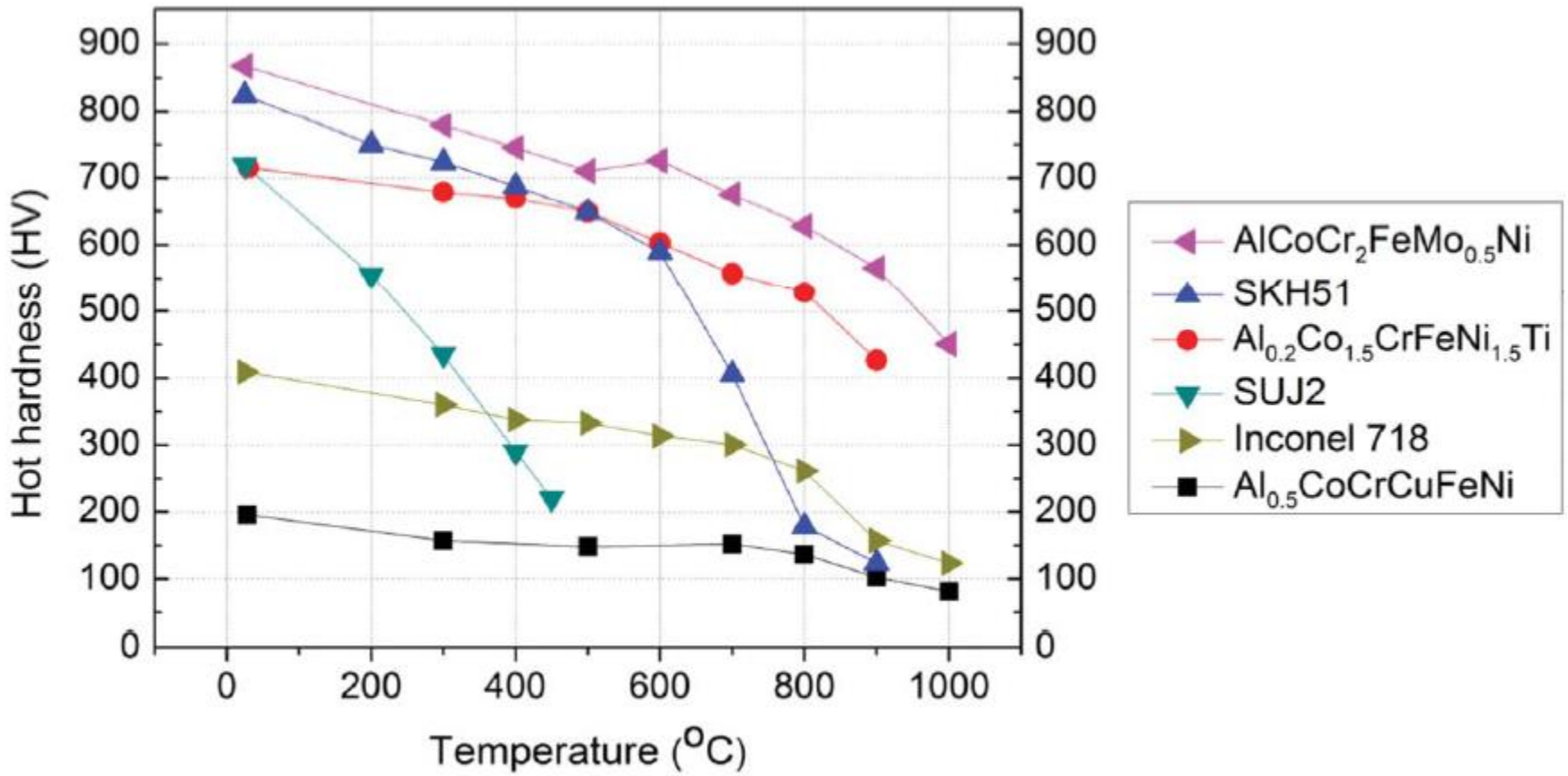

Hardness of various alloys as function of temperature

1. Chuang MH, Tsai MH, Wang WR, Lin SJ, Yeh JW. Microstructure and wear behavior of AlxCo1.5CrFeNi1.5Tiy high-entropy alloys. Acta Mater. 2011;59:6308–6317.
2. Hsu CY, Juan CC, Wang WR, Sheu TS, Yeh JW, Chen SK.On the superior hot hardness and softening resistance of AlCoCr*x*FeMo0.5Ni high-entropy alloys. Mater Sci Eng A. 2011;528:3581–3588.

High temperature performance

Low diffusion rate & High transition temperature & reduced driving force to eliminate defects

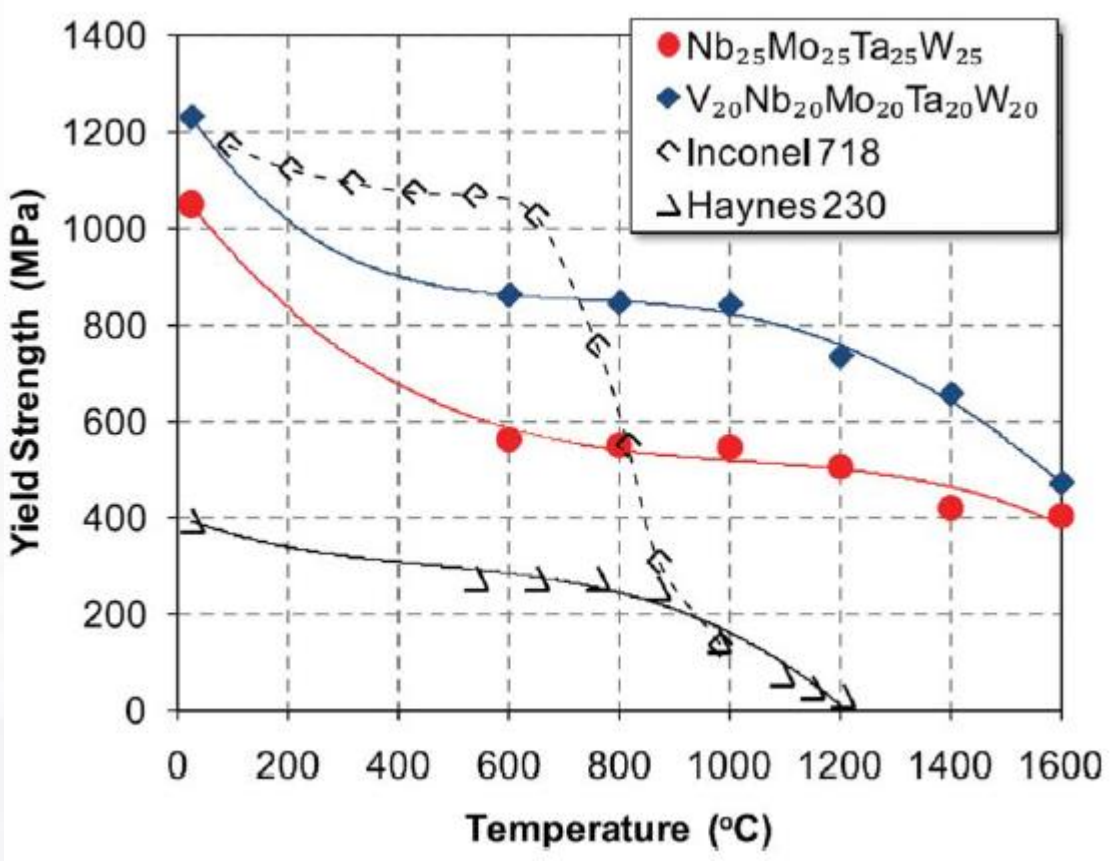

Yield strength as functions of temperature for the $Nb_{25}Mo_{25}Ta_{25}W_{25}$ and$V_{20}Nb_{20}Mo_{20}Ta_{20}W_{20}$ alloys and two superalloys.

Senkov ON,Wilks GB, Scott JM, Miracle DB. Mechanical properties of Nb25Mo25Ta25W25 and V20Nb20Mo20Ta20W20 refractory high entropy alloys. Intermetallics. 2011;19:698–706

Synthesis Methods of HEA

- **Liquid state: Arc melting, induction melting, Bridgman solidification**
- **Solid state: High-energy ball mill**
- **Gas state: Sputtering or molecular beam epitaxy (MBE)**
- **Other methods: thermal spray, laser cladding, electrodeposition**

Mechanical properties of HEA

- **Hardness and strength**
- **Wear and fatigue**
- **Fracture**
- **Creep**
- **Compression and tensile deformation**

Strengthening mechanism

1. Solid solution strengthening
2. Grain size strengthening
3. Twinning
4. Etc.

Typical strengthening mechanism of HEAs

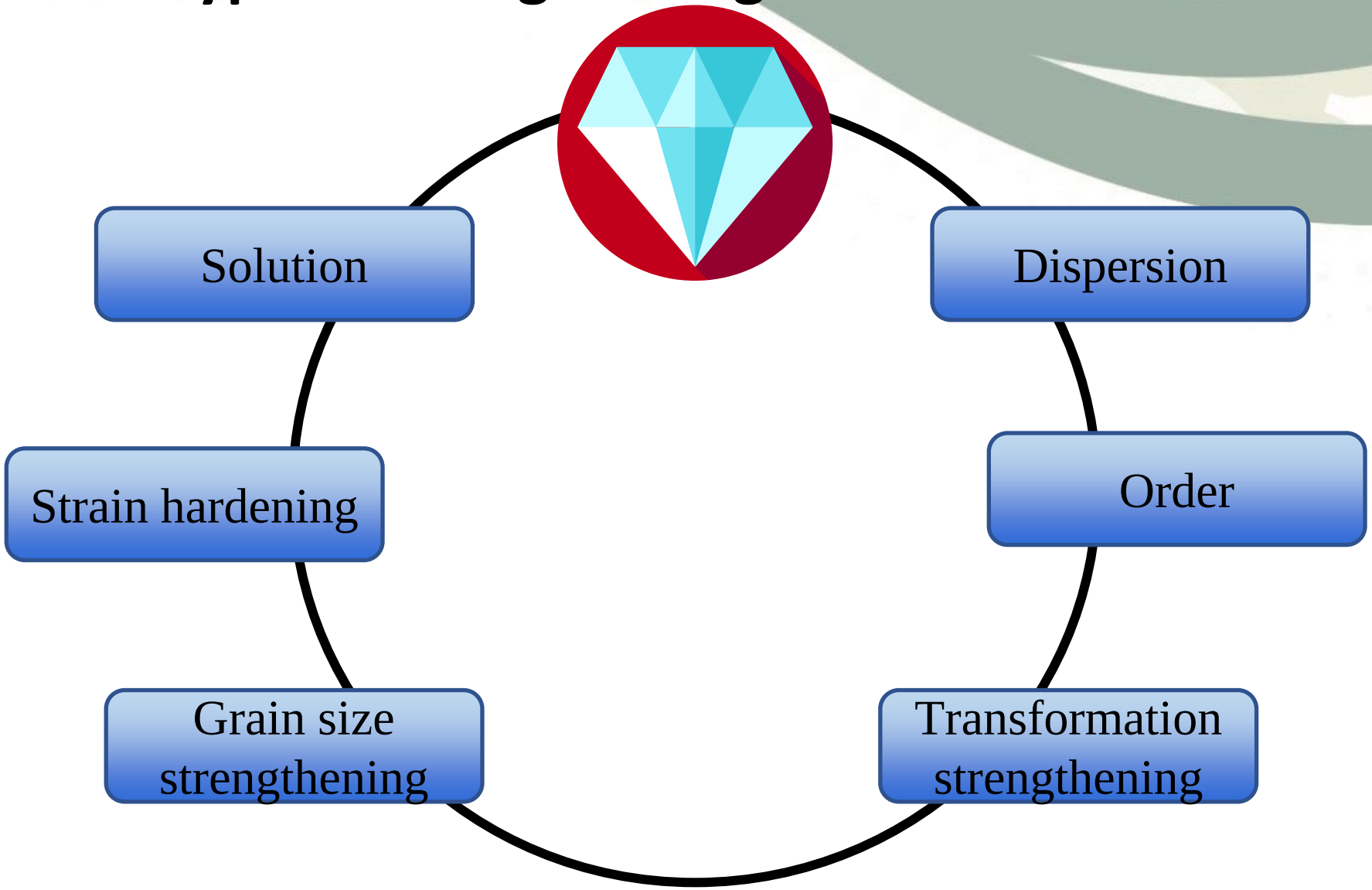

Elastic constant of HEA

- **Temperature dependence of elastic modulus G & E of Cantor alloy**
- **Normal behavior**

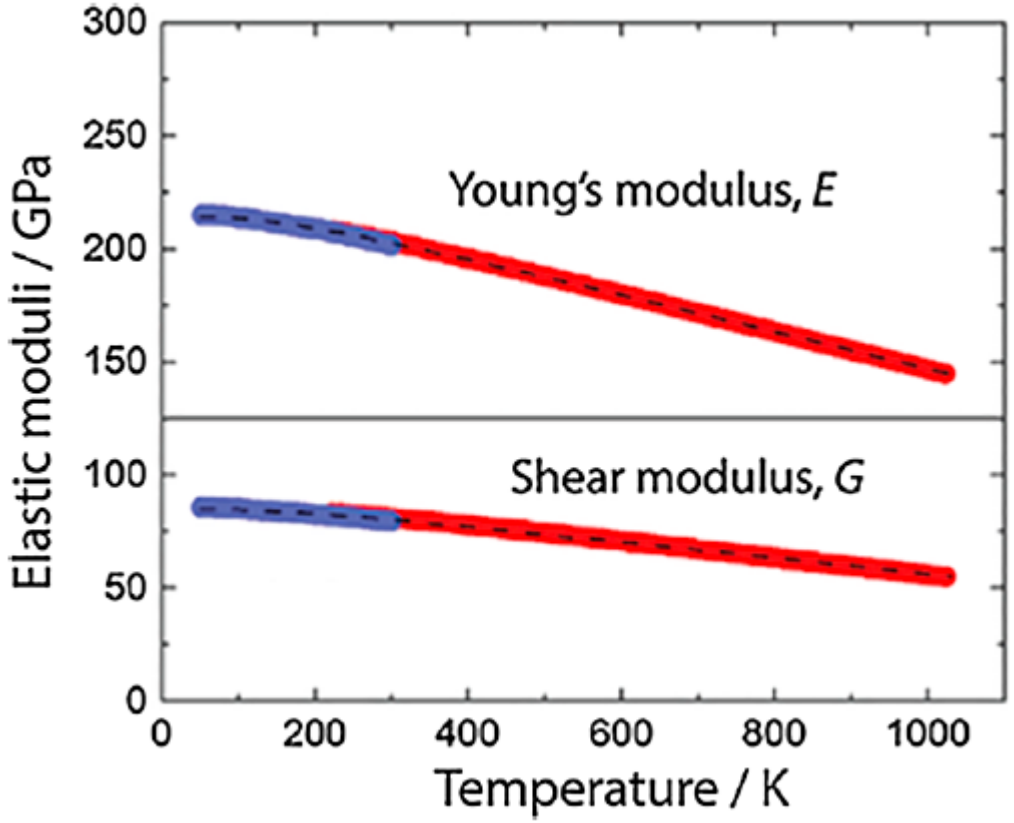

Resonant ultrasonic spectroscopy (RUS) frequency technique

T=298K，$G = 85GPa$
$E = 214GPa$

Calculation of E & G of Cantor alloy (Varshni expression): $G = 85 - 16/(e^{\frac{448}{T}} - 1)$, $E = 214 - 35/(e^{\frac{416}{T}} - 1)$

Haglund, A., Koehler, M., Catoor, D., George, E. P., & Keppens, V. (2015). Polycrystalline elastic moduli of a high-entropy alloy at cryogenic temperatures. *Intermetallics*, *58*, 62-64.

Wear performance of HEAs

$$W_r = \frac{L}{\Delta V}$$

$\Delta V = Volume\ loss$, $L =$ sliding distance

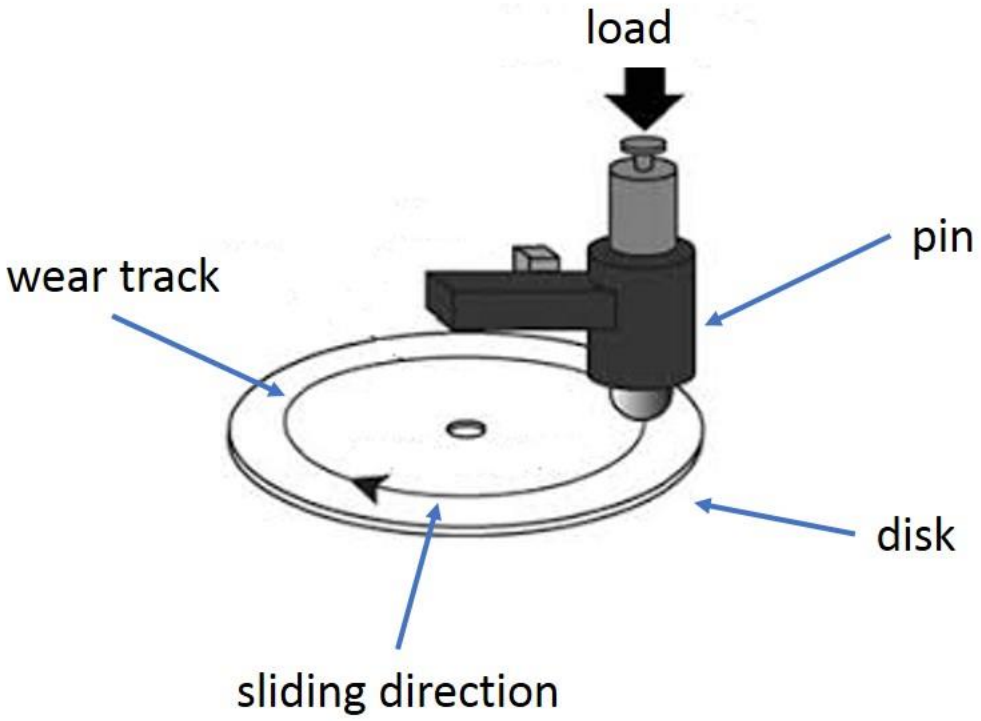

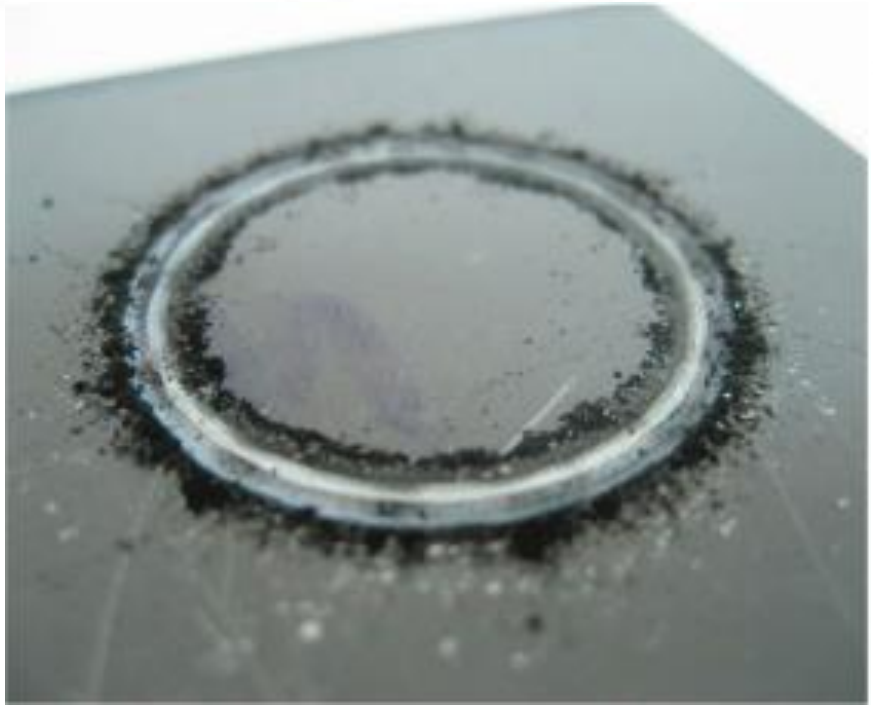

Pin on disk test

1. Laurence W. McKeen, in Fluorinated Coatings and Finishes Handbook (Second Edition), 2016
2. https://www.tribonet.org/wiki/pin-on-disk-test/

Wear performance of HEAs

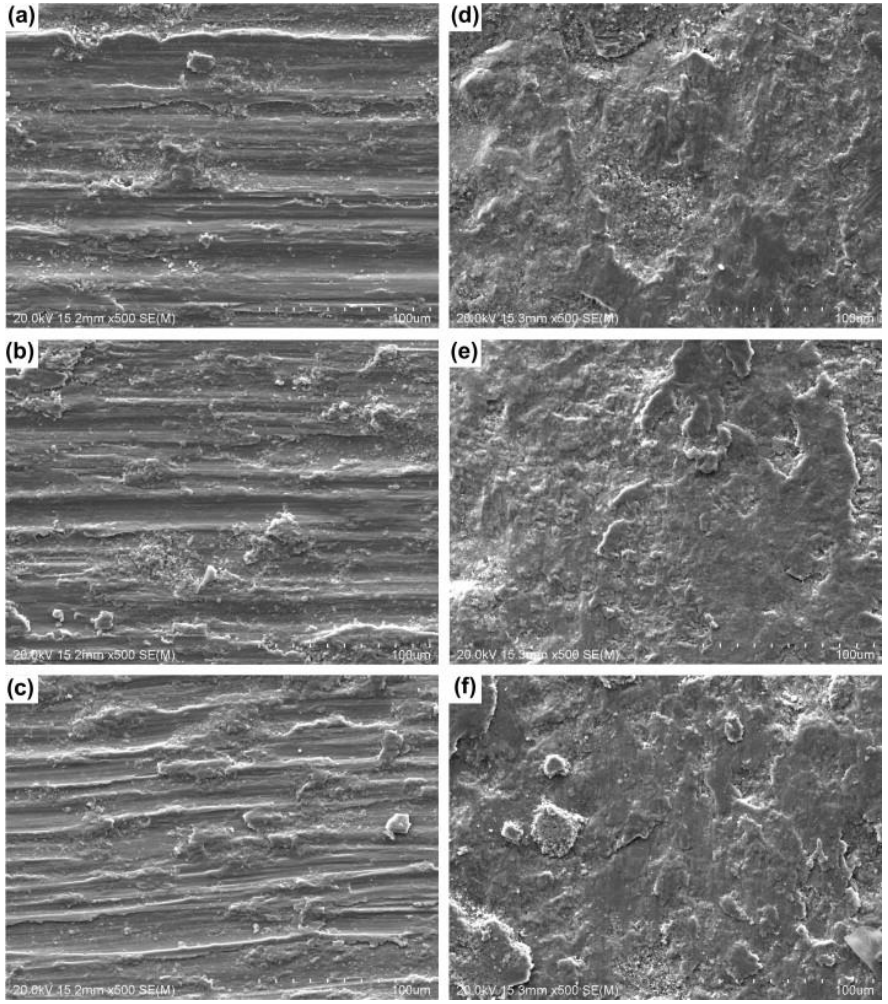

Adhesive wear & severe abrasive wear

Oxidation, less weight loss (Heat generate)

Surface morphology of two alloys

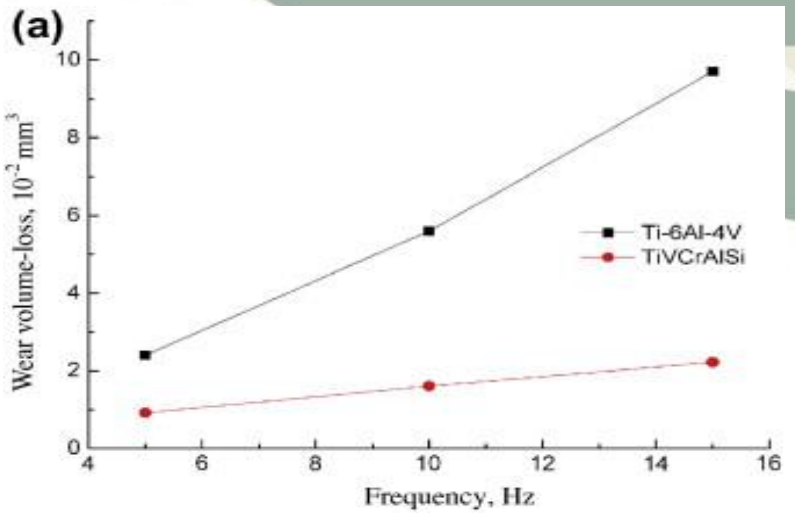

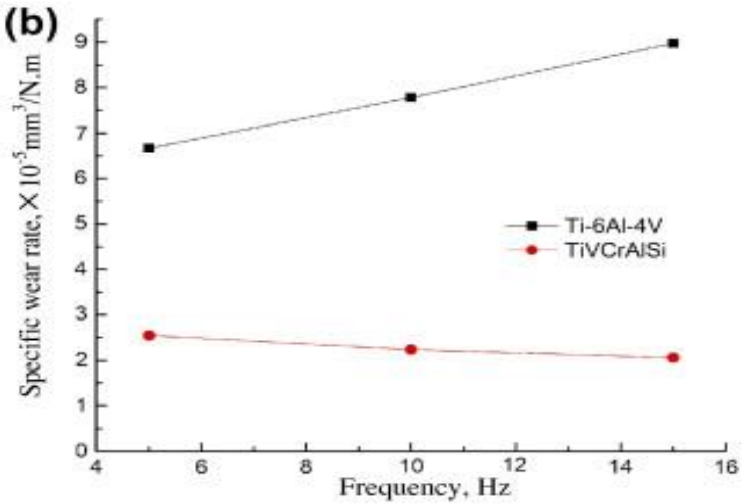

Volumetric loss vs. Frequency

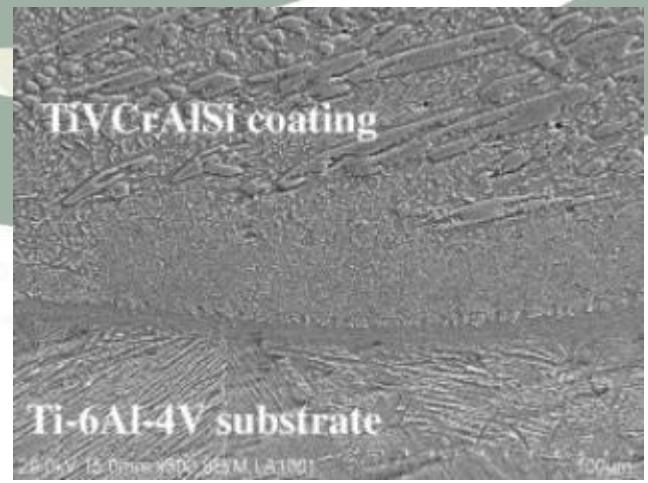

Hardness & wear resistance:

$(Ti,V)_5Si_3$ and bcc phase solid solution

Thermal conductivity & wear resistance

Friction coefficient

Huang, C., Zhang, Y., Vilar, R., & Shen, J. (2012). Dry sliding wear behavior of laser clad TiVCrAlSi high entropy alloy coatings on Ti–6Al–4V substrate. Materials & Design, 41, 338-343.

Wear performance of HEAs

HEA is a promising candidate as anti-wear alloys due to excellent work hardening ability

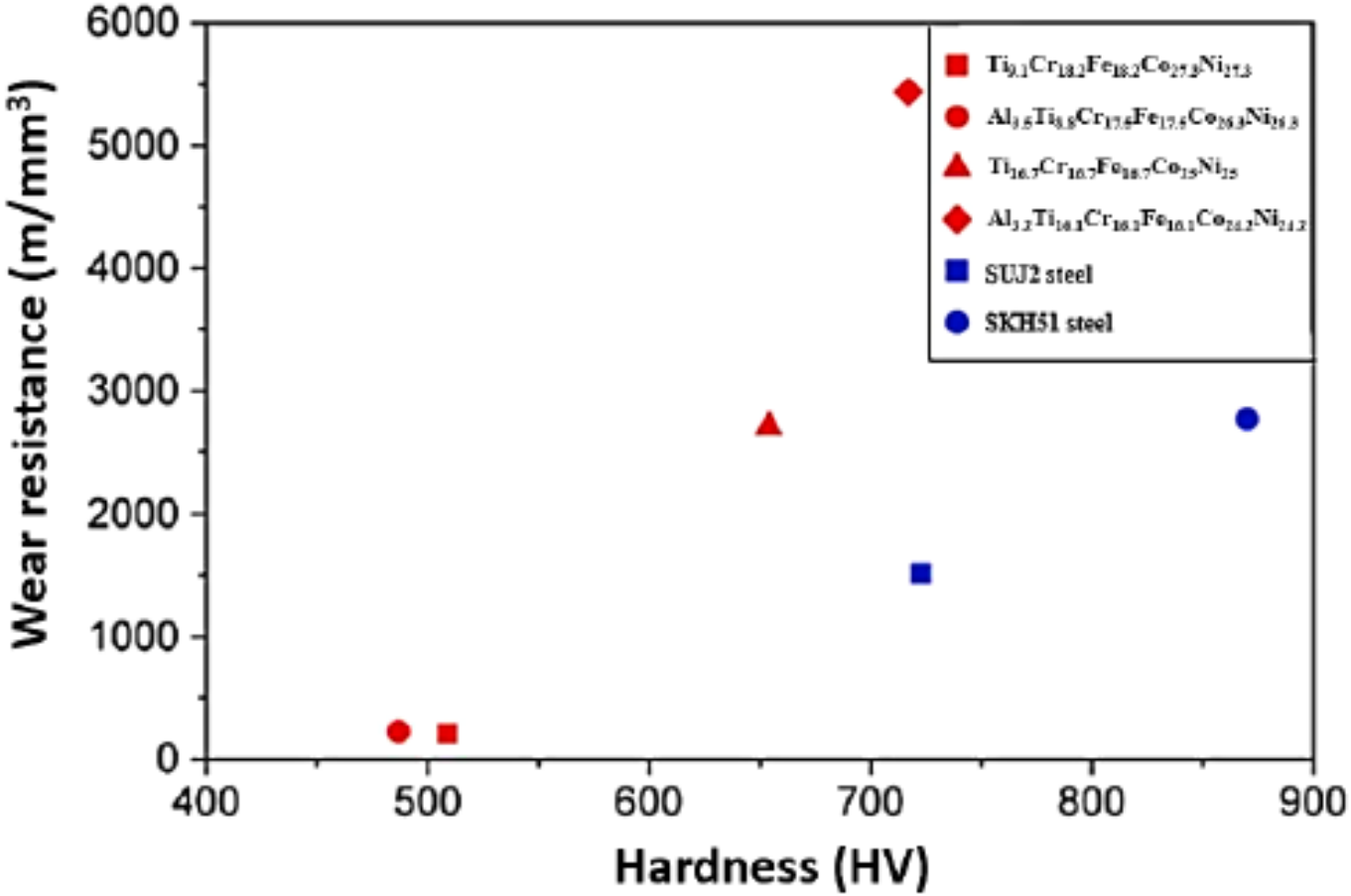

Wear resistance behavior as a function of hardness

Chuang M-H, Tsai M-H, Wang W-R, Lin S-J, Yeh J-W. Microstructure and wear behavior of AlxCo1.5 CrFeNi1.5Tiy high-entropy alloys. Acta Materialia 2011;59:6308¨C17.

Fracture toughness

Stress intensity factor: K_{1c}

$$J_{1c} = \frac{K_{1c}^2}{E'} = \lambda \delta_{1c} \sigma_0$$

$$E' = E \ (Plane\ stress)$$

$$E' = \frac{E}{1-\nu} \ (Plane\ strain)$$

Intrinsic (plasticity): microcracks, voids…
Extrinsic (shielding): inelastic zones, bridging, sliding…

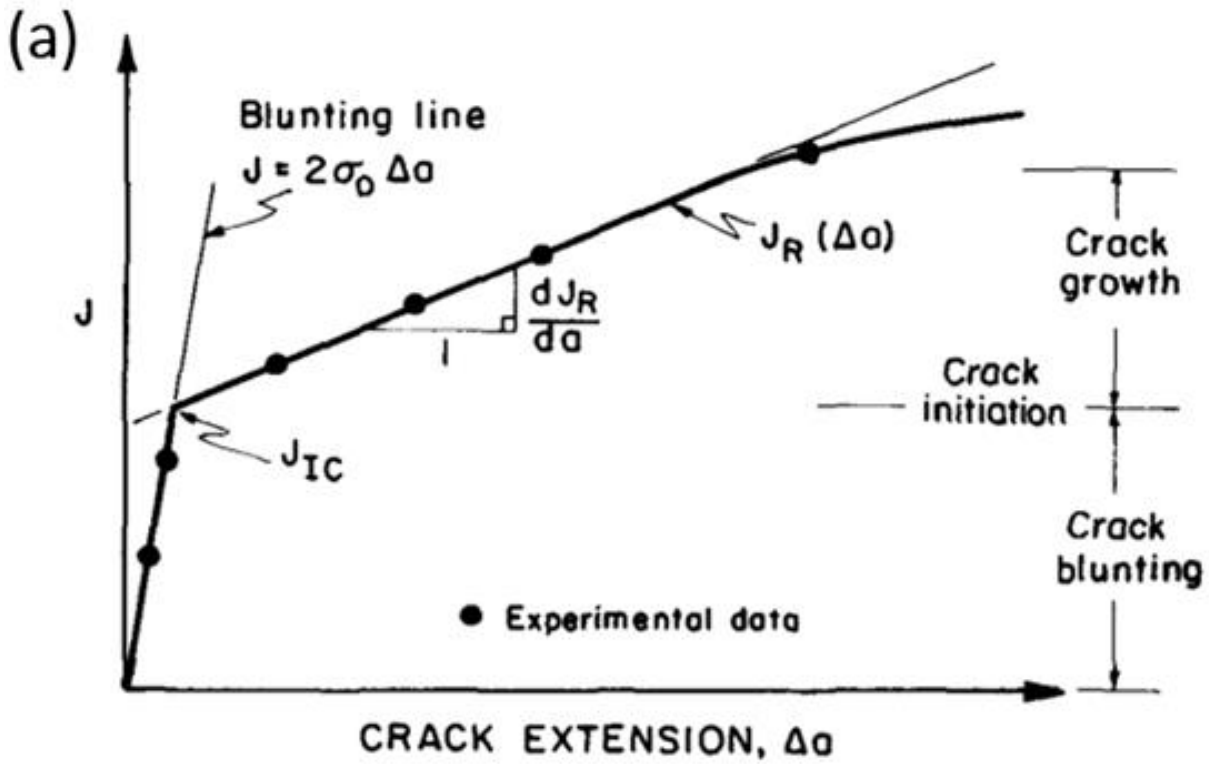

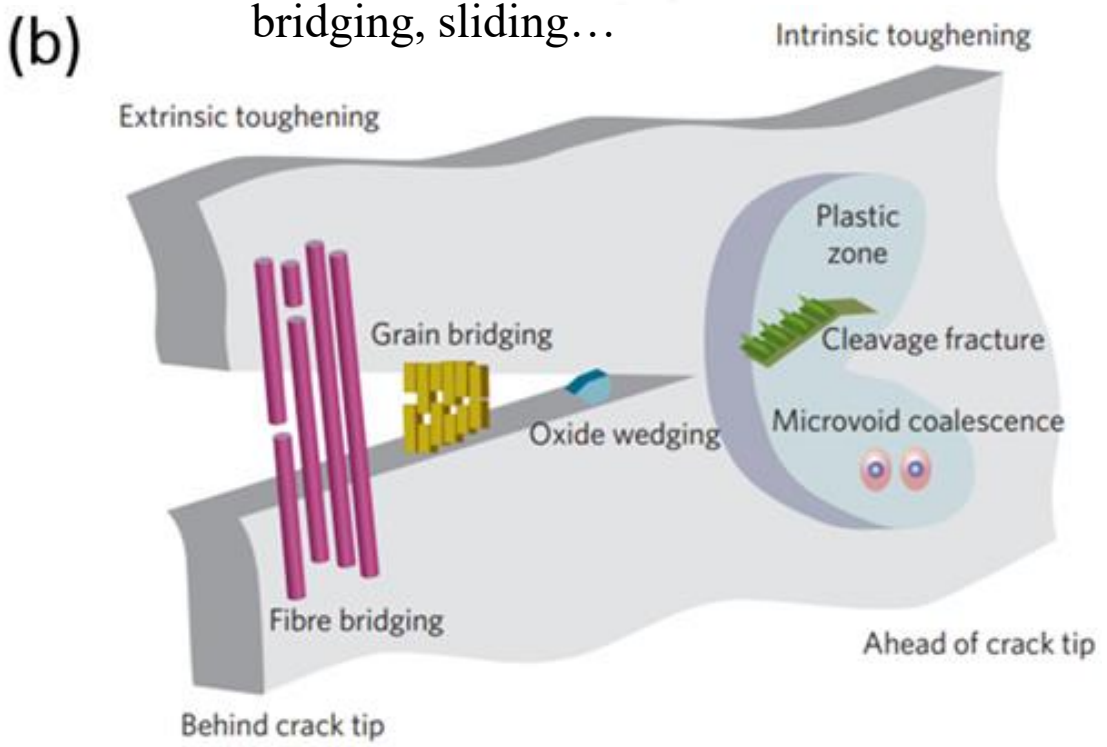

Ritchie RO, Thompson AW. On macroscopic and microscopic analyses for crack initiation and crack growth toughness in ductile alloys. Metall Trans A 1985;16:233¨C48.

Fracture toughness

Cantor alloy

77K	$J_{1c} = 255kJ/m^2$	$K_{1c} = 219MPa \cdot m^{\frac{1}{2}}$
200K	$J_{1c} = 260kJ/m^2$	$K_{1c} = 221MPa \cdot m^{\frac{1}{2}}$
293K	$J_{1c} = 250kJ/m^2$	$K_{1c} = 217MPa \cdot m^{\frac{1}{2}}$

a

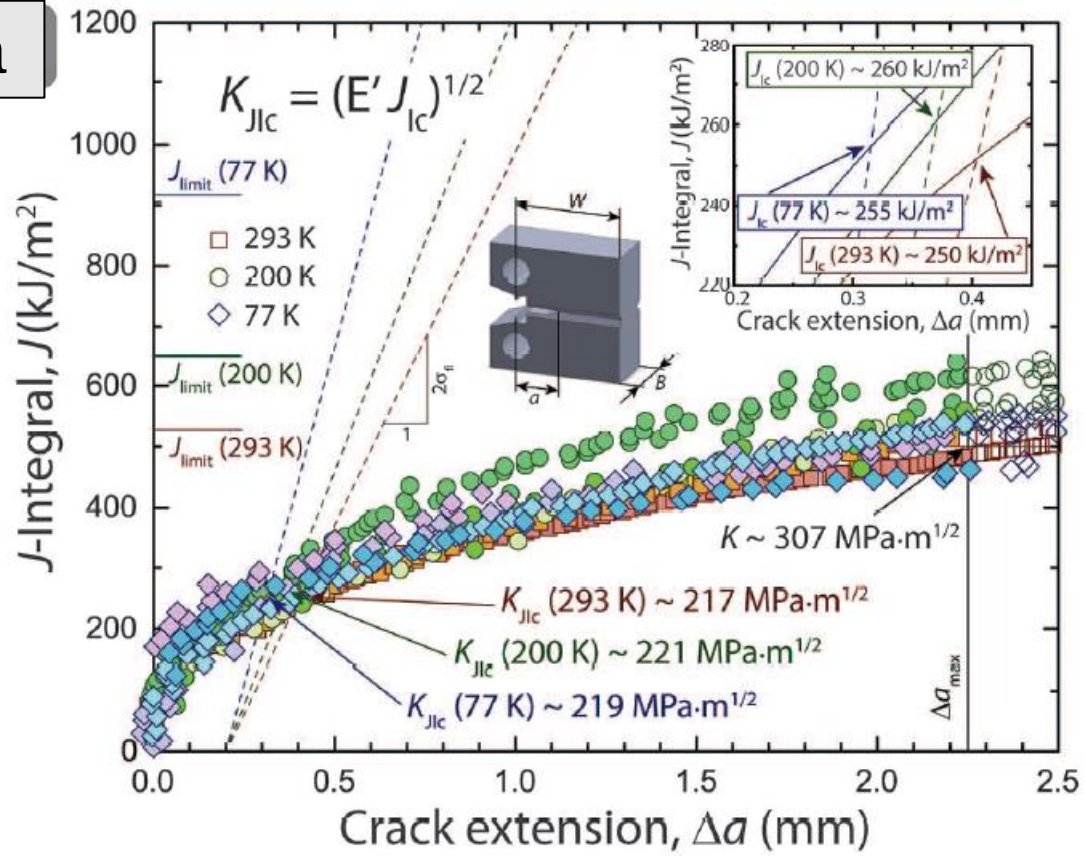

b

Temperature dependence of strength and toughness

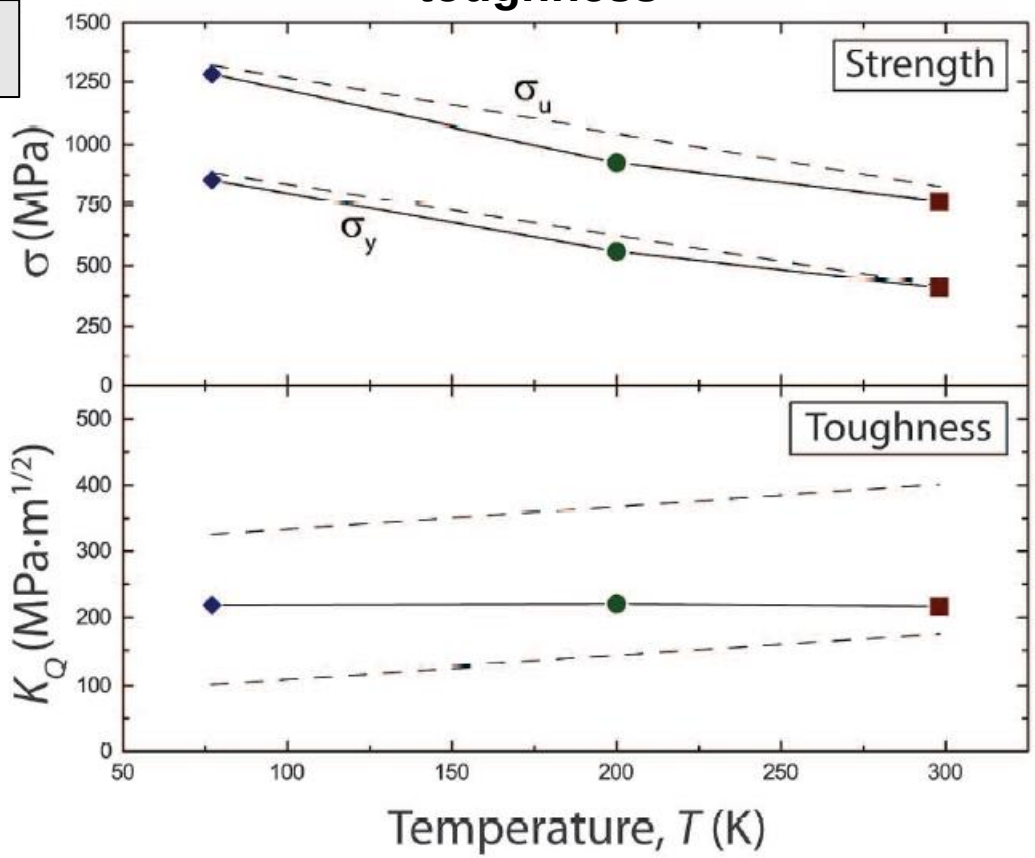

Fracture toughness of Cantor alloy at different temperature (77K, 200K, 217K)

Gludovatz, B., Hohenwarter, A., Catoor, D., Chang, E. H., George, E. P., & Ritchie, R. O. (2014). A fracture-resistant high-entropy alloy for cryogenic applications. Science, 345(6201), 1153-1158.

Fracture toughness

- Annealing twins
- Dislocation
- Nanotwins

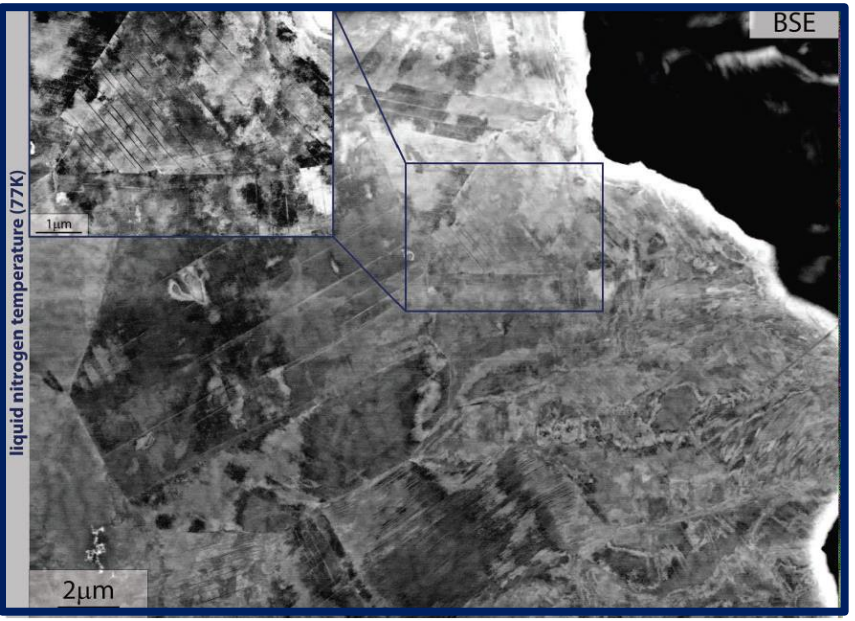

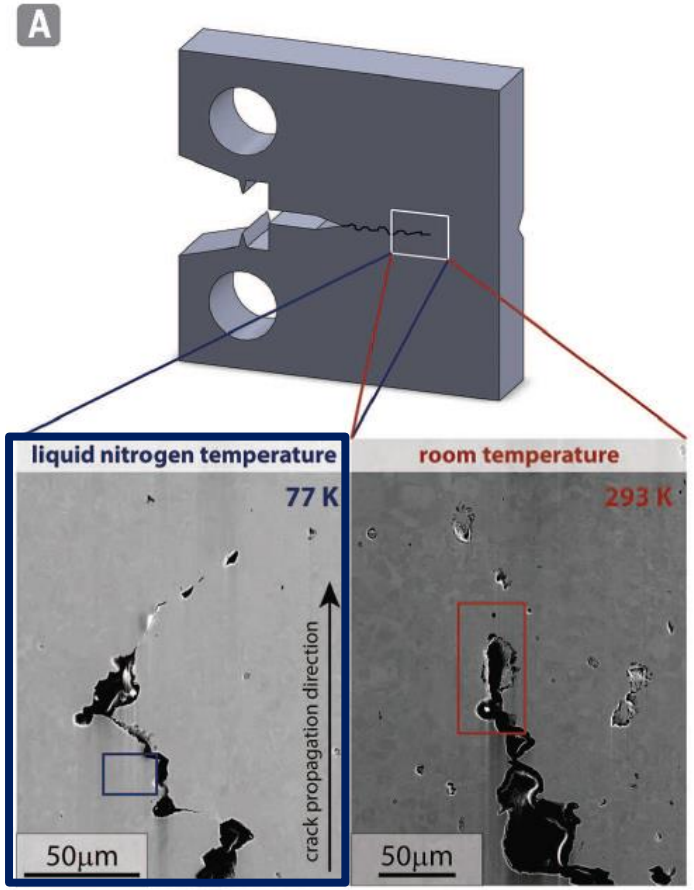

SEM images of crack tip

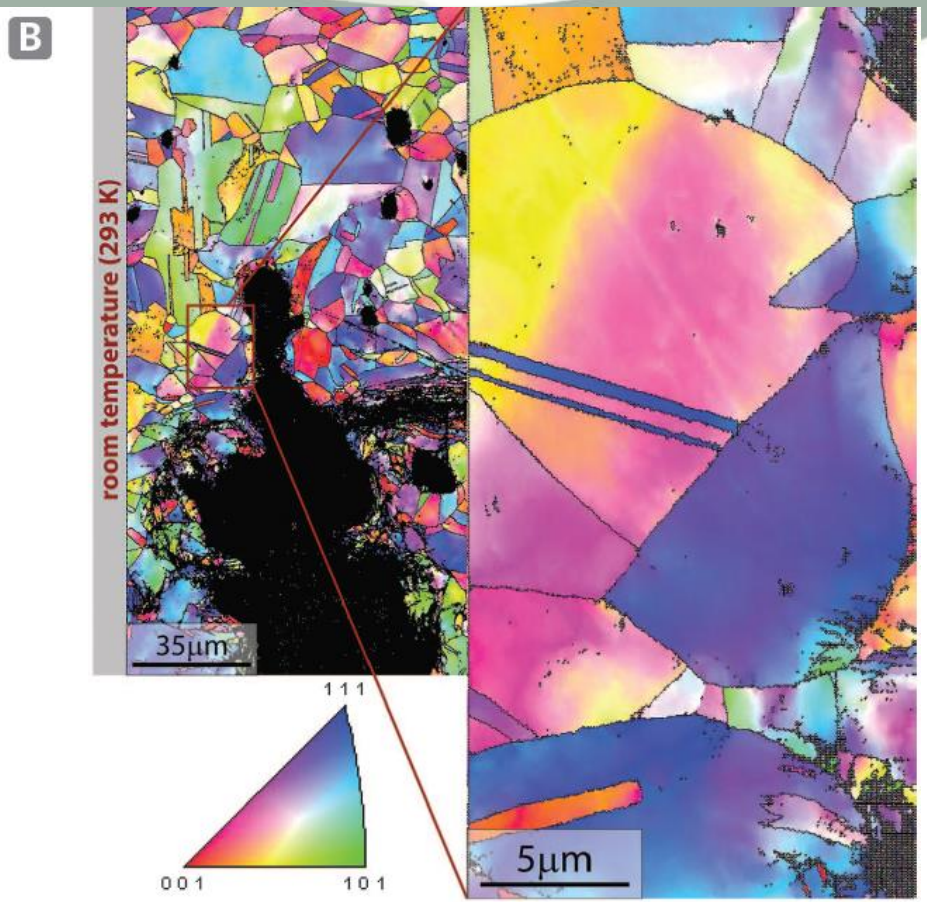

EBSD images of crack tip

Gludovatz, B., Hohenwarter, A., Catoor, D., Chang, E. H., George, E. P., & Ritchie, R. O. (2014). A fracture-resistant high-entropy alloy for cryogenic applications. Science, 345(6201), 1153-1158.

Grain size strengthening

Growth kinetic constant: $C = A_0 \exp\left(-\frac{Q}{RT}\right)$

Q: activation energy for grain growth at absolute temperature T

A_0: material constant

$d^n - d_0^n = Ct$ **(d: grain size, t: time)**

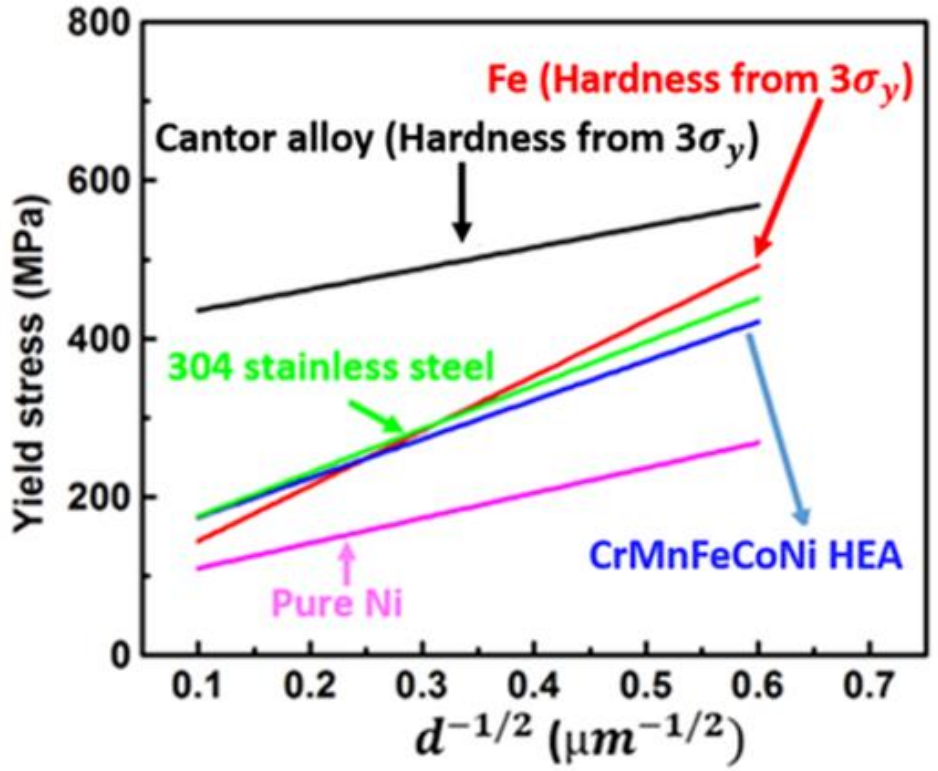

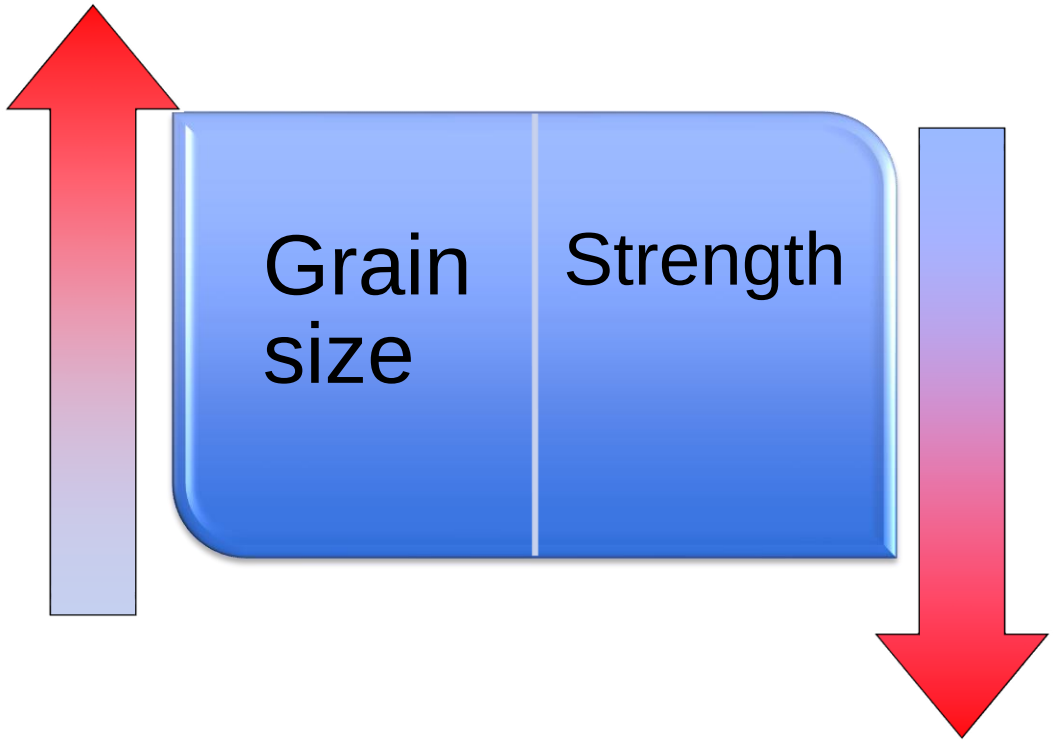

Li, Z., Zhao, S., Ritchie, R. O., & Meyers, M. A. (2019). Mechanical properties of high-entropy alloys with emphasis on face-centered cubic alloys. *Progress in Materials Science*, *102*, 296-345.

Creep

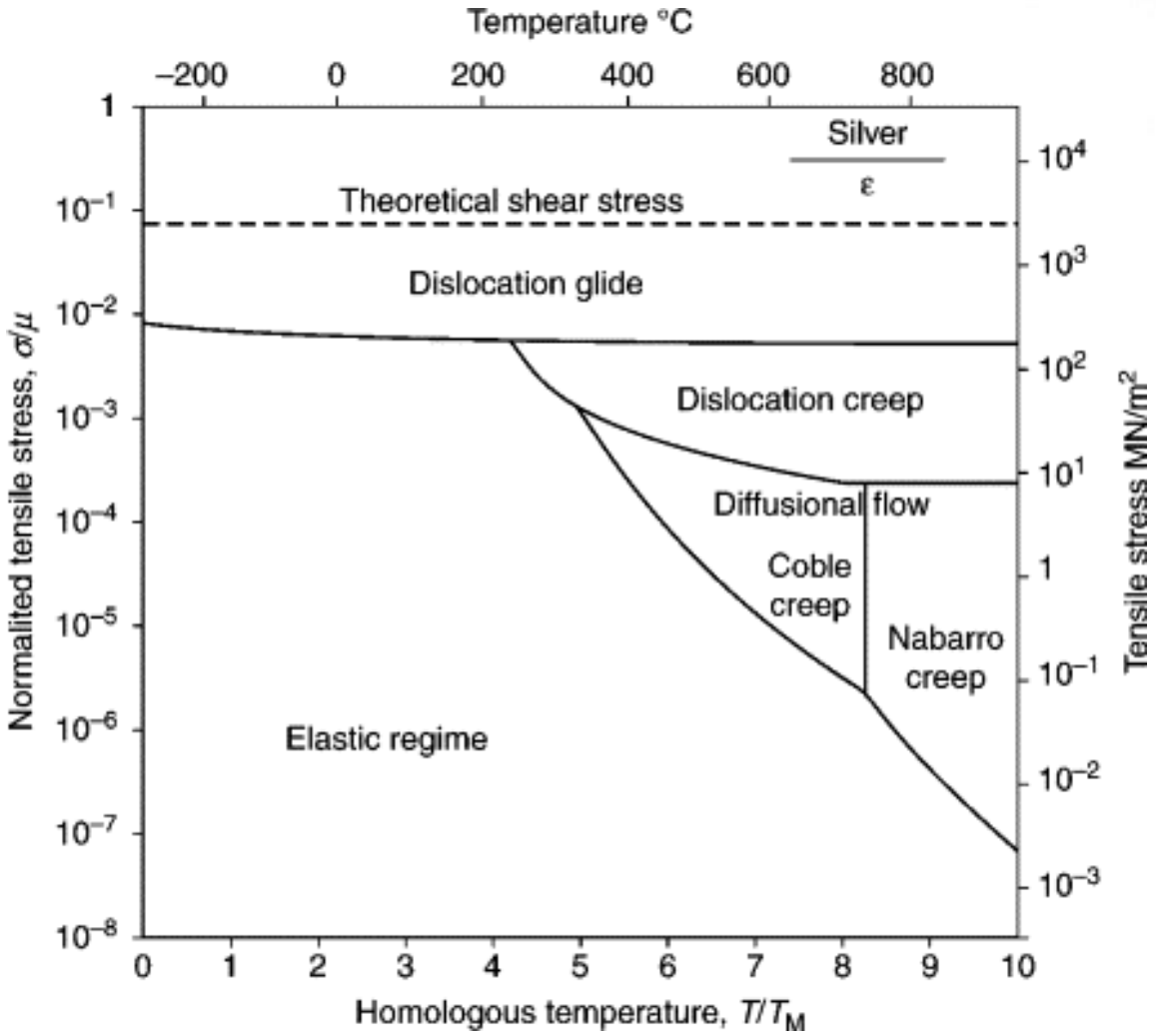

Weertman–Ashby map

Main creep mechanism

1. **Above the theoretical: shear strength: Plastic flow of the material could occur without dislocation involved.**

2. $\frac{\sigma}{G} > 10^{-2}$**, Below the theoretical shear strength: dislocation glide**

3. $10^{-5} < \frac{\sigma}{G} < 10^{-2}$**: Dislocation glide & climb**

4. $\frac{\sigma}{G} \leq 10^{-5}$**: diffusion creep**

Herring-Nabarro
Vacancies migrate from one grain cell to another. (diffusion creep)

Murty, K. L., Gollapudi, S., Ramaswamy, K., Mathew, M. D., & Charit, I. (2013). Creep deformation of materials in light water reactors (LWRs). In Materials Ageing and Degradation in Light Water Reactors (pp. 81-148). Woodhead Publishing.

Creep

1. **Transient curve vs. inverted transient curve (stress dependence of creep mechanisms)**
   Creep stress component: $n = \partial \dot{\varepsilon}_{SS} / \partial ln\sigma$
2. **Creep rate< 10^{-5}**
   Low stress dependence (higher applied stresses)
   High stress dependence (Lower applied stresses)

3. **Temperature dependence**

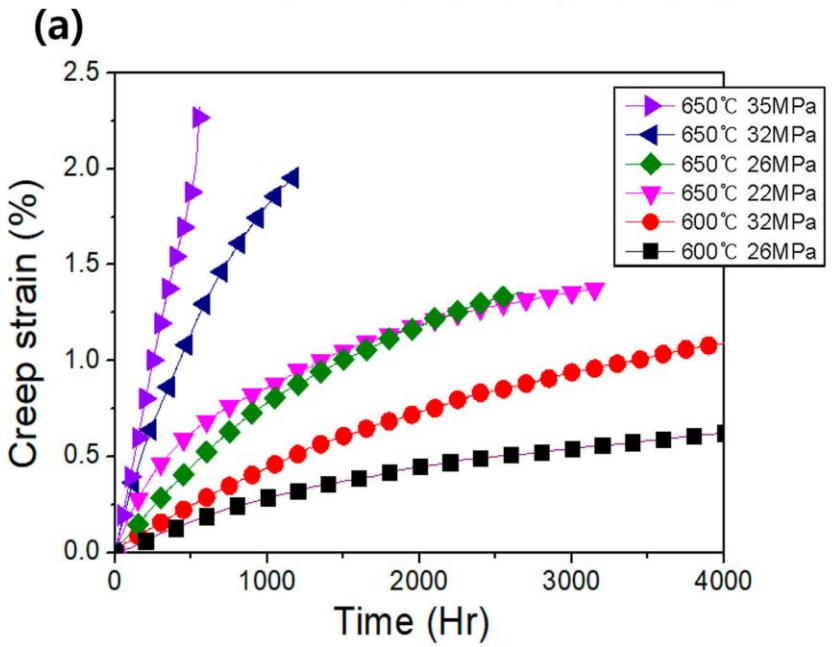

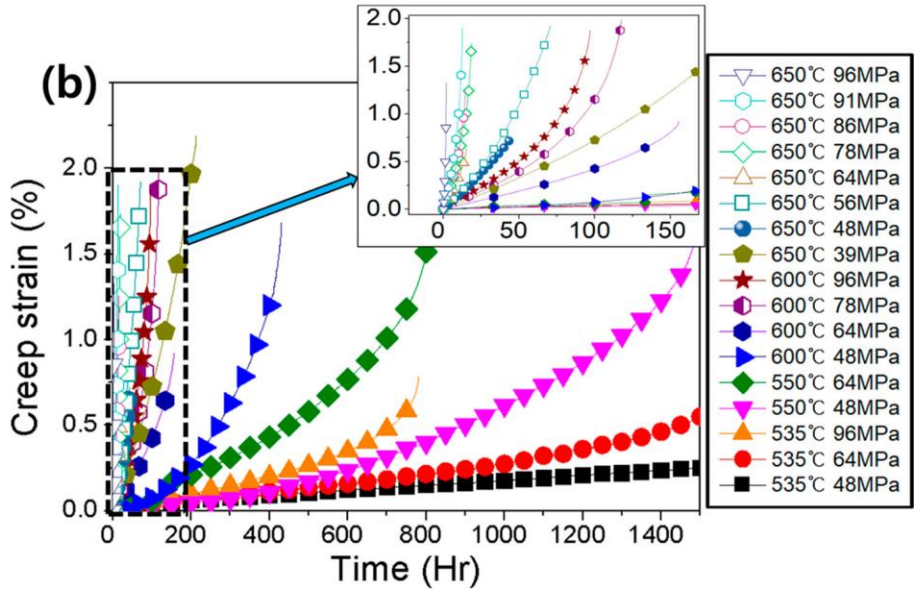

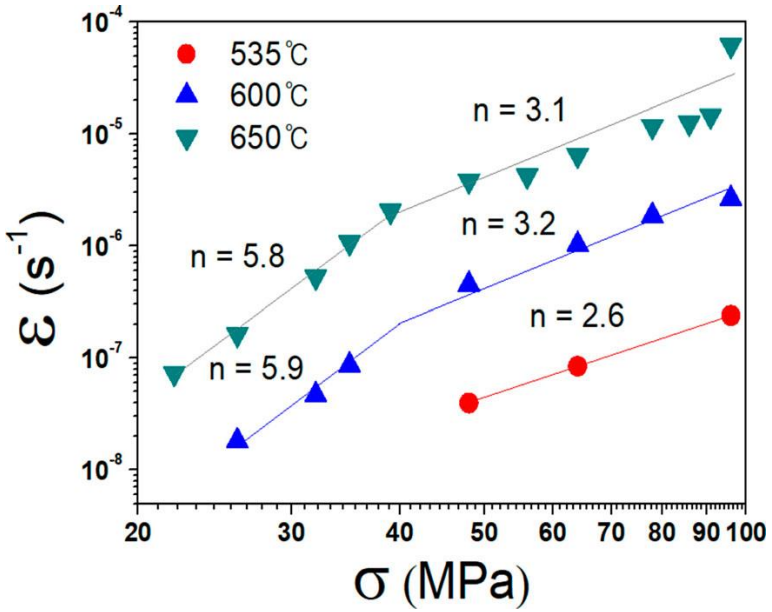

Sluggish diffusion

Lattice distortion

Stress dependence of the steady state creep rate of CoCrFeMnNi.

Creep curves of CoCrFeMnNi HEA at temperatures between 535°C and 650°C. (a) lower stresses and (b) high stresses.

Kang, Y. B., Shim, S. H., Lee, K. H., & Hong, S. I. (2018). Dislocation creep behavior of CoCrFeMnNi high entropy alloy at intermediate temperatures. Materials Research Letters, 6(12), 689-695.

Strain hardening of HEAs

Considère criterion: $\frac{d\sigma}{d\varepsilon} = \sigma$ (Necking)

High work hardening rate, high flow stress, high toughness

(Mechanical twinning, solid solution…)

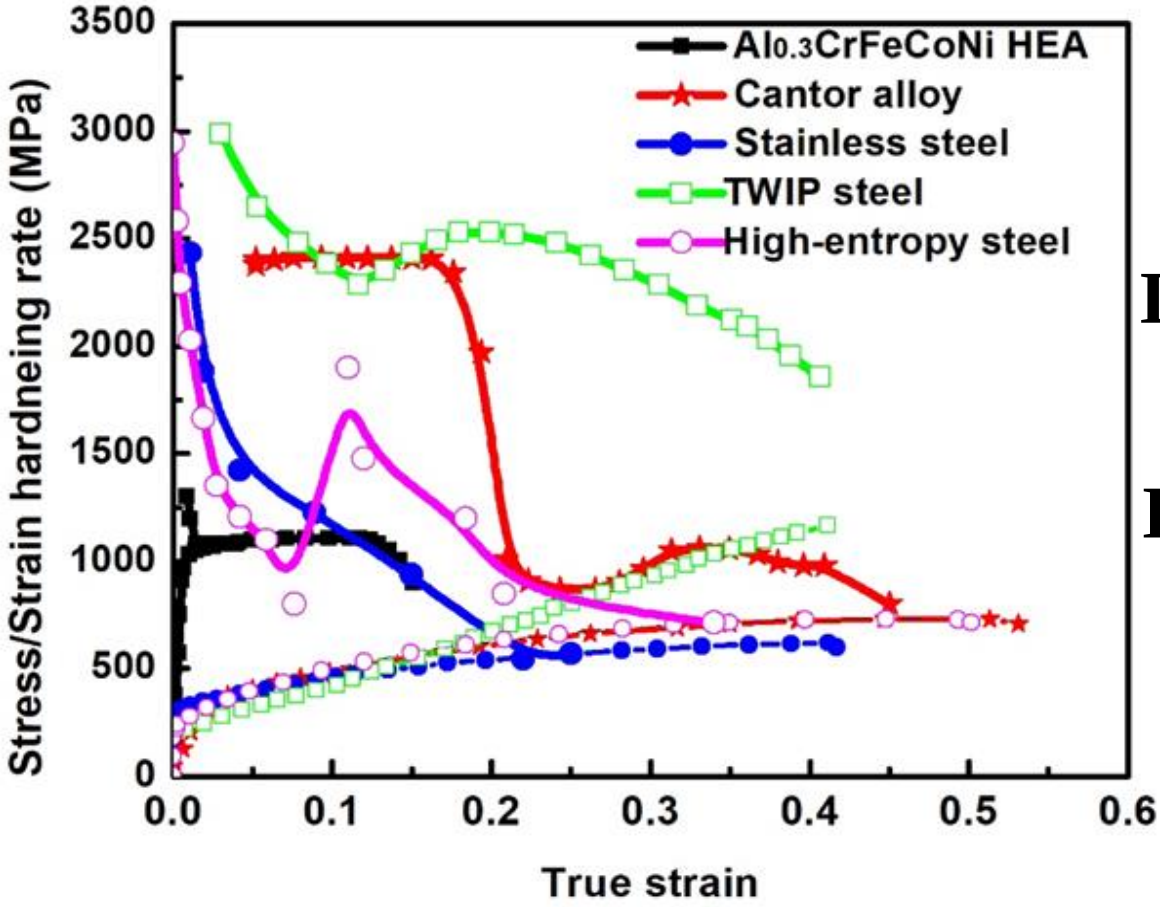

Low $\frac{d\sigma}{d\varepsilon}$: Readily neck

High $\frac{d\sigma}{d\varepsilon}$: High toughness

Li, Z., Zhao, S., Ritchie, R. O., & Meyers, M. A. (2019). Mechanical properties of high-entropy alloys with emphasis on face-centered cubic alloys. *Progress in Materials Science*, *102*, 296-345.

Strength and ductility trade off

Ductility

Strength

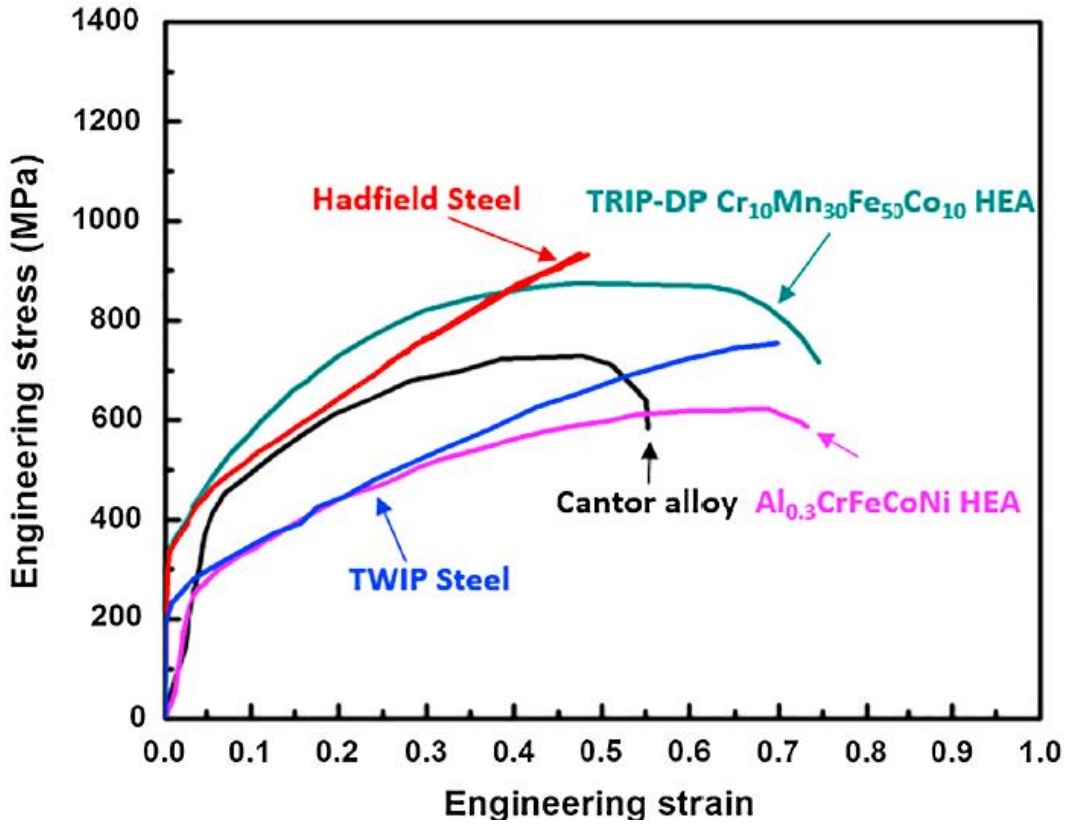

Li Z, Pradeep KG, Deng Y, Raabe D, Tasan CC. Metastable high-entropy dual-phase alloys overcome the strength–ductility trade-off. Nature 2016;534:227–30

Twinning effect

$$\sigma_T = \alpha_T \left(\frac{\gamma_{SF}}{G b_s}\right)^{\frac{1}{2}} \text{ (Twinning stress)}$$

Insensitive to temperature

Zerilli-Armstrong equation: $\sigma_S = \sigma_G + C_2 \exp\left[-\left(C_3 - C_4 \ln\left(\frac{\dot{\varepsilon}}{\dot{\varepsilon}_0}\right) T\right] + k_s d^{-\frac{1}{2}}$

α_T: adjustable parameter

γ_{SF}: stacking fault energy

$\gamma_{SF} \sim 25 mJ/m^2$

$a_0 \sim 0.36 nm$

Strain rate decrease, temperature increase

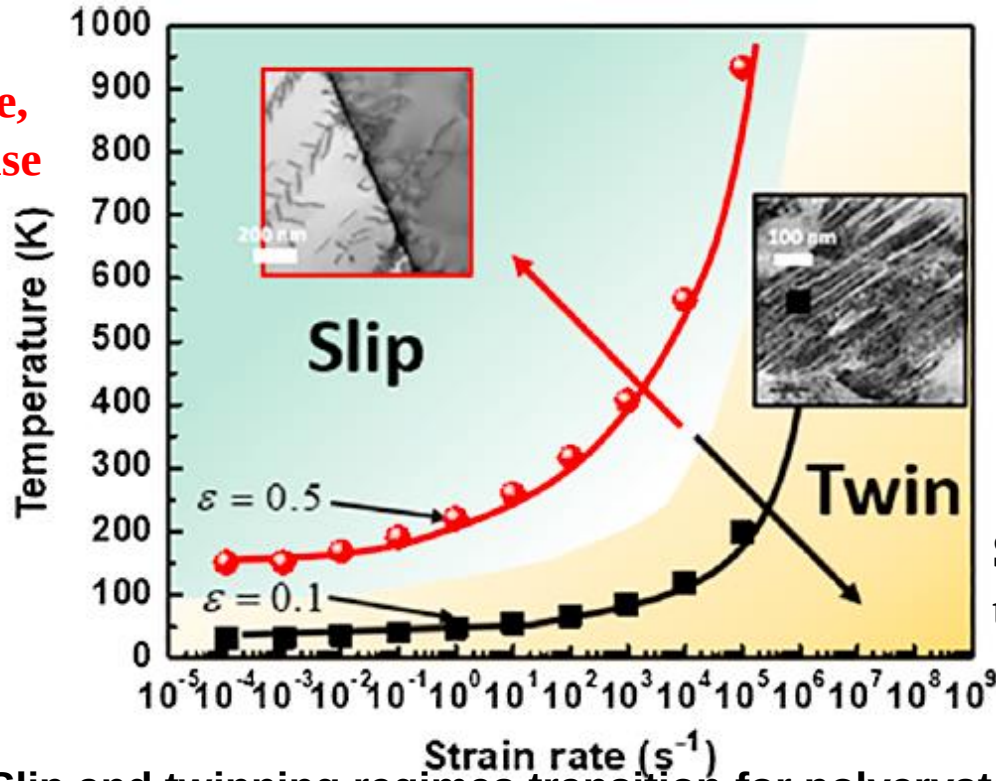

Strain rate increase, temperature decrease

Slip and twinning regimes transition for polycrystalline CrMnFeCoNi Cantor alloy with grain size ~50 μm at two levels of plastic strain

Meyers MA, Vöhringer O, Lubarda VA. The onset of twinning in metals: a constitutive description. Acta Materialia 2001;49:4025–39.

Twinning effect

Twin evolution in Cantor alloy (77K) (tensile)

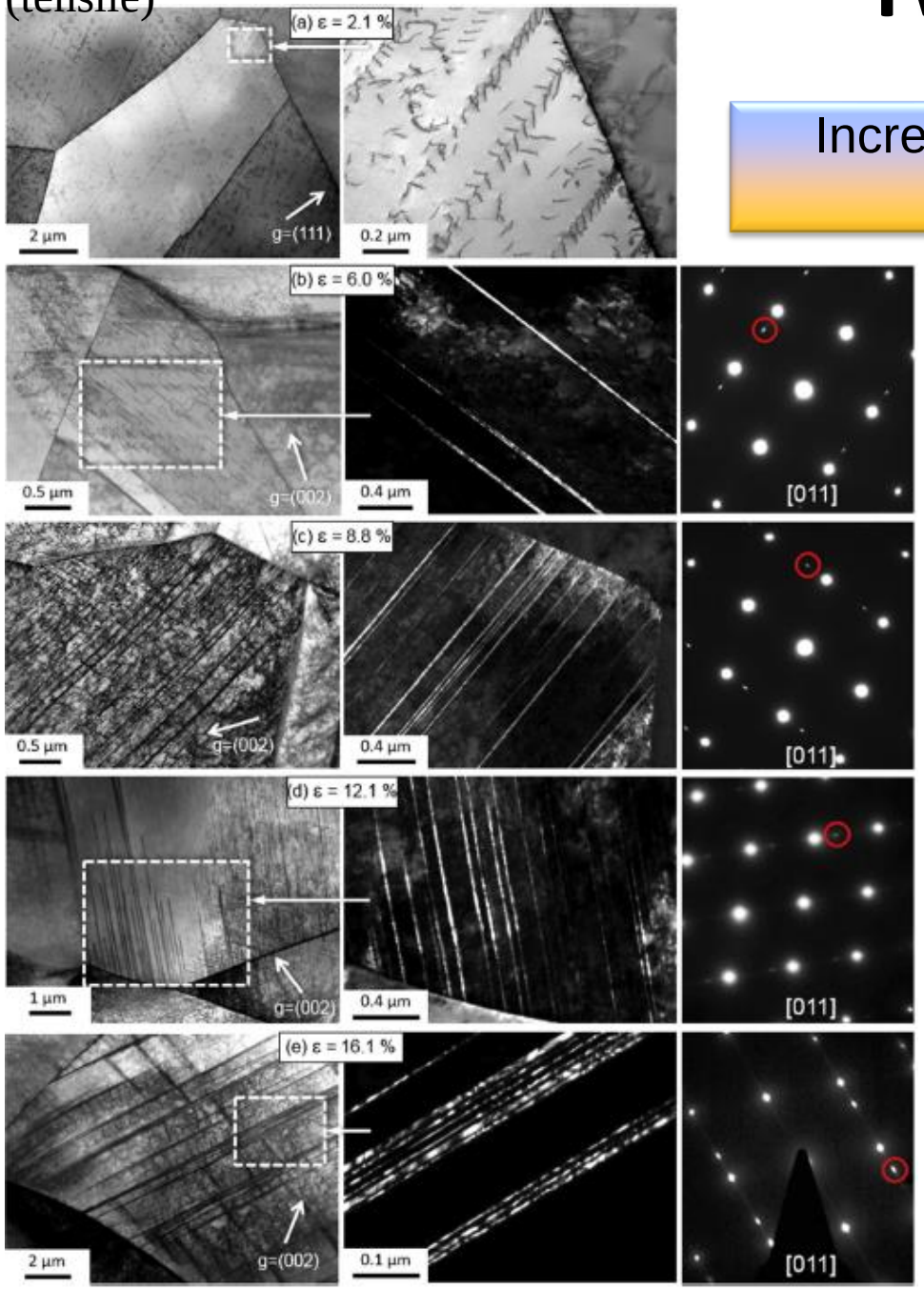

Increase in dislocation density

Initiation of nanotwins

Volume fraction of twin increases

$$\sigma_T \approx 700MPa$$
$$\alpha_T \approx 16GPa$$

Intersecting twins

Laplanche G, Gadaud P, Horst O, Otto F, Eggeler G, George E. Temperature dependencies of the elastic moduli and thermal expansion coefficient of an equiatomic, single-phase CoCrFeMnNi high-entropy alloy. J Alloys Compd 2015;623:348–53.

Twinning-induced plasticity (TWIP)

1. Major hardening mechanism of stainless steel
2. Twinning does not contribute primary effect at room temperature tensile deformation in Cantor alloy.
3. Reducing Ni to lower SFE with four component system.
4. Reducing Co, Cr contents.

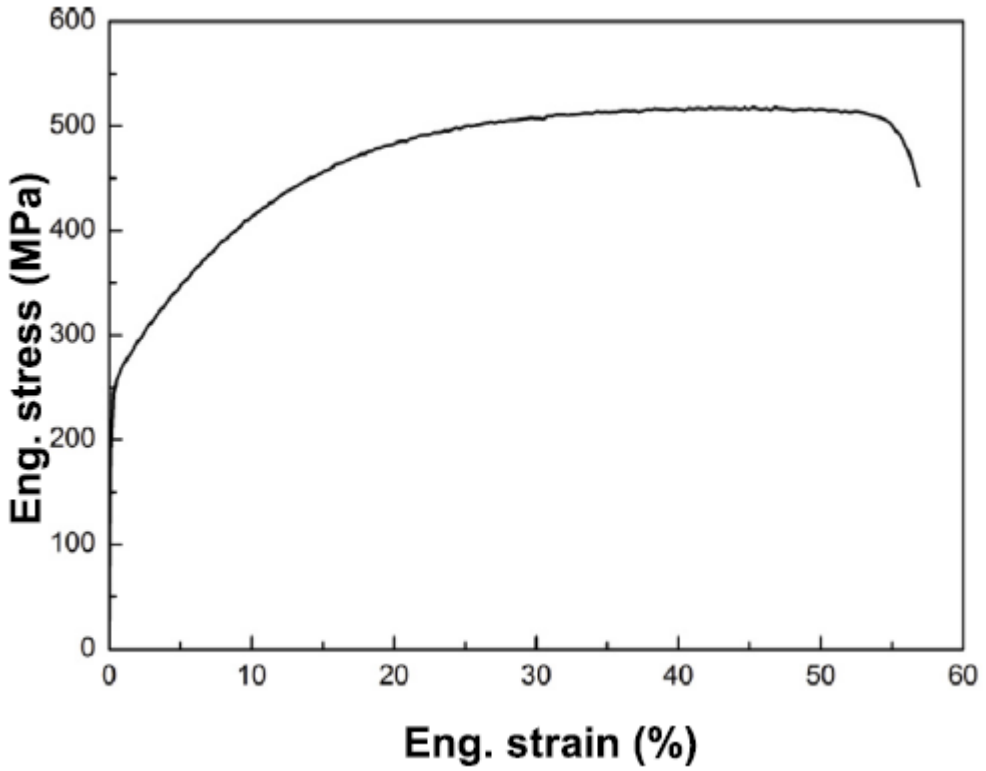

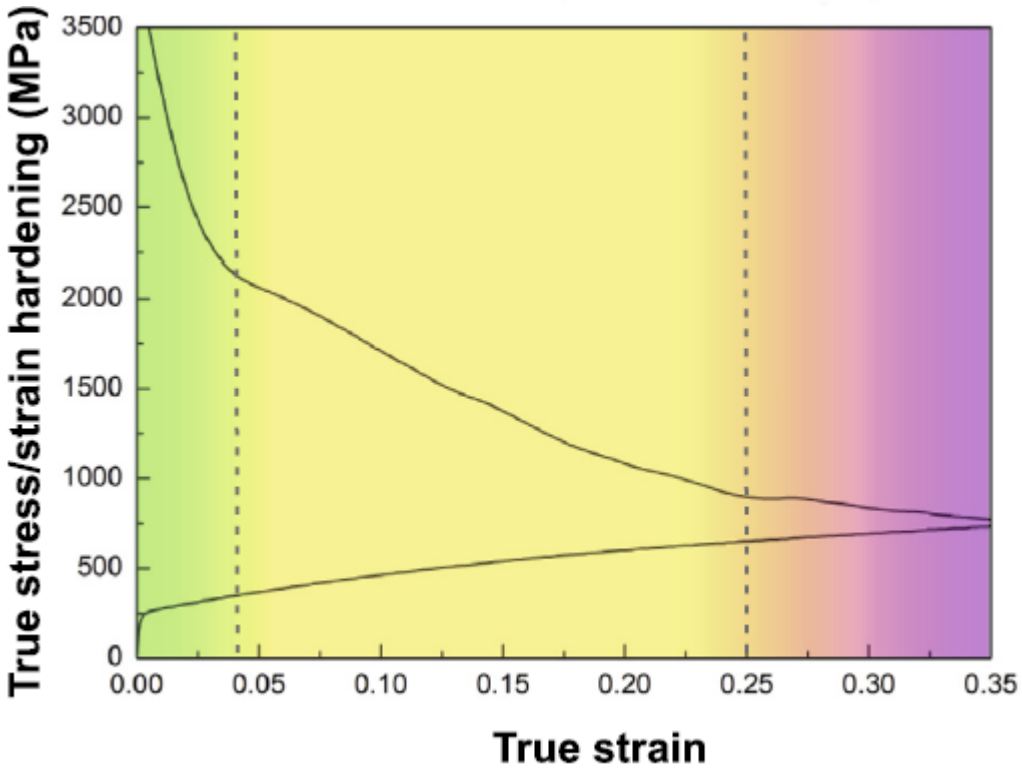

Deng, Y., Tasan, C. C., Pradeep, K. G., Springer, H., Kostka, A., & Raabe, D. (2015). Design of a twinning-induced plasticity high entropy alloy. Acta Materialia, 94, 124-133.

Twinning-induced plasticity (TWIP)

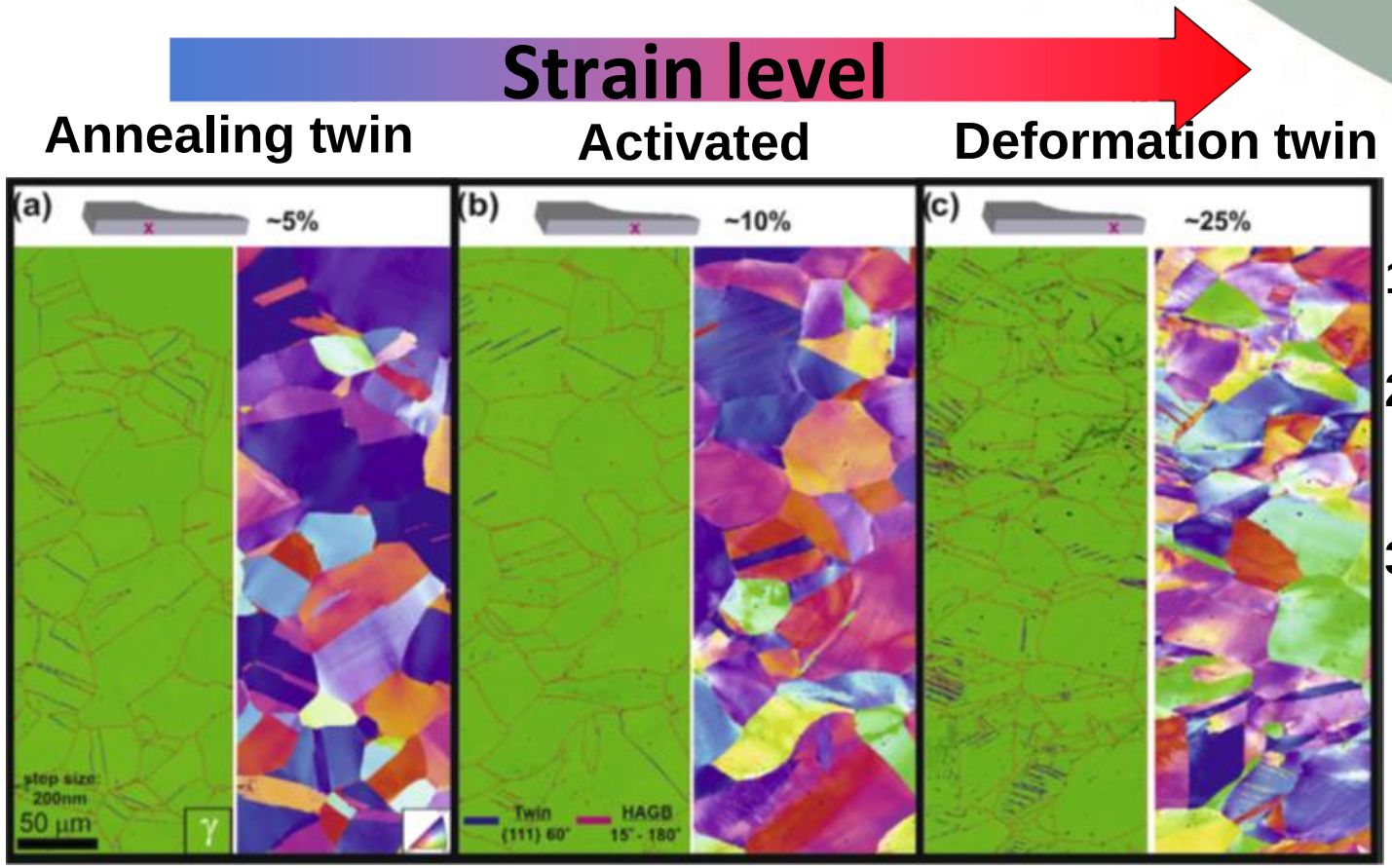

1. Deformation twin activated (~10%)
2. Work hardening by impeding movement of dislocation
3. Strain level increases, fraction of twin boundaries increase

EBSD and IPF images at cross section of the deformed $Fe_{40}Mn_{40}Co_{10}Cr_{10}$ sample at varied strain level

Twin HAGB

Deng, Y., Tasan, C. C., Pradeep, K. G., Springer, H., Kostka, A., & Raabe, D. (2015). Design of a twinning-induced plasticity high entropy alloy. Acta Materialia, 94, 124-133.

Fatigue

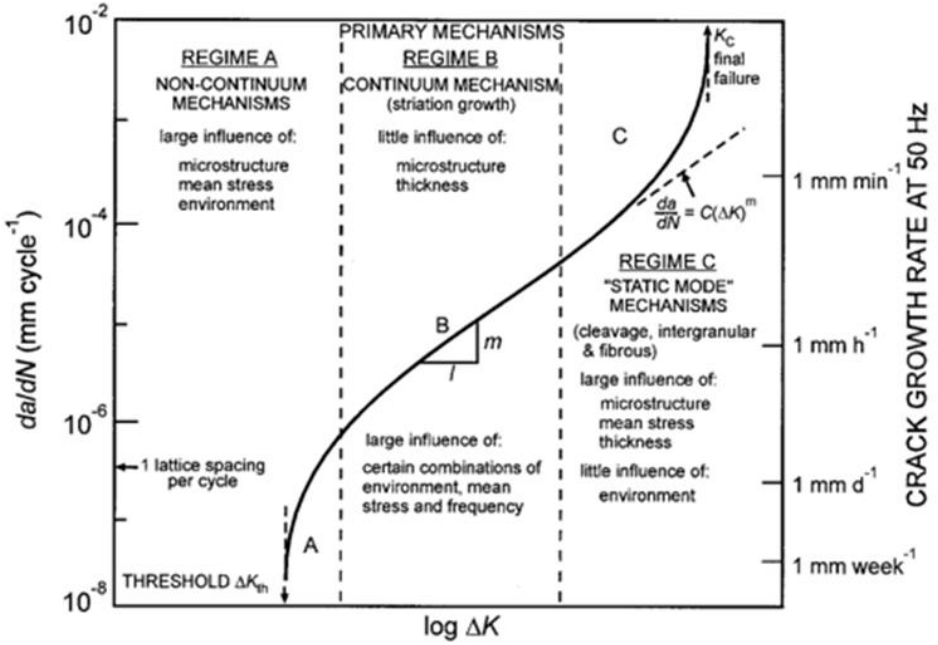

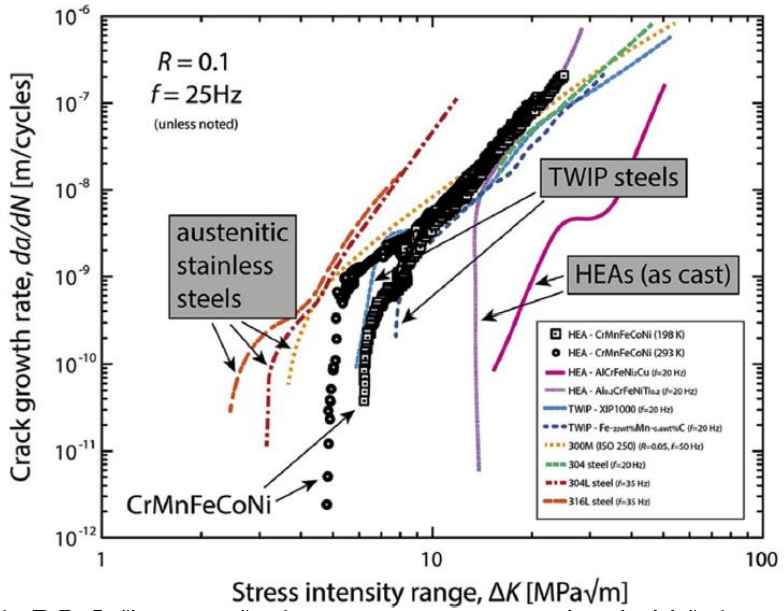

Fatigue crack growth:

$$\frac{da}{dN} = f[\Delta K, K_{max}(or\ R), v, enviornment, waveform \dots]$$

Stress intensity range:

$$\Delta K = K_{max} - K_{min}$$

$$\frac{da}{dN} = C(\Delta K)^m$$

C & m: material scaling constant (2~4 for metal)

K: stress intensity

Four stages of fatigue:

- **Initial cyclic damage (cyclic softening or hardening)**
- **Generation of initial flaw**
- **Macroscopic propagation of flaw**
- **Catastrophic failure**

1. Ritchie RO. Influence of microstructure on near-threshold fatigue-crack propagation in ultra-high strength steel. Met Sci 1977;11:368–81.
2. Thurston KV, Gludovatz B, Hohenwarter A, Laplanche G, George EP, Ritchie RO. Effect of temperature on the fatigue-crack growth behavior of the high-entropy alloy CrMnFeCoNi. Intermetallics 2017;88:65–72.

Fatigue 2

Fractographic analysis of CrMnFeCoNi samples tested at 293K and 198K.

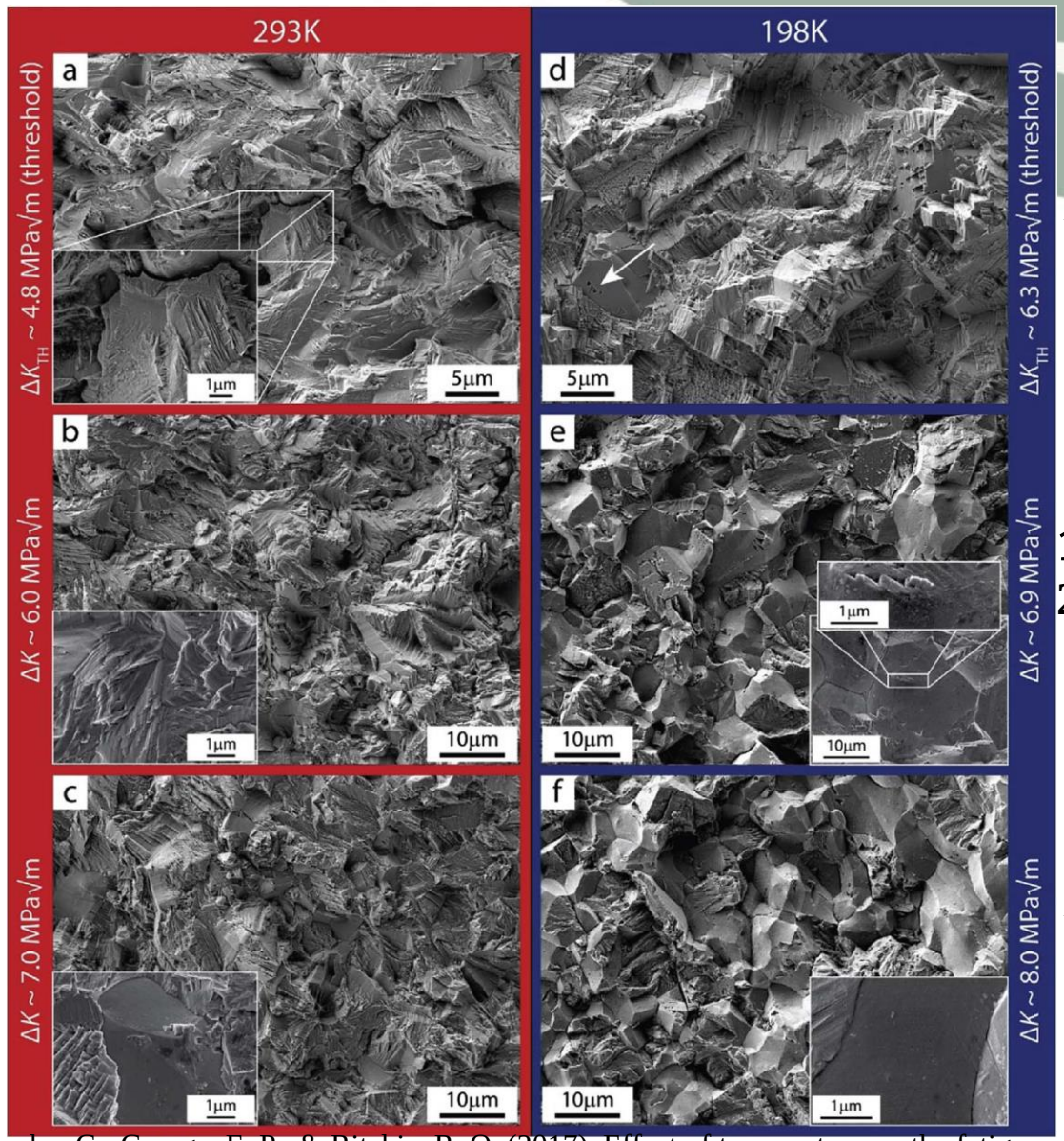

No twins
Planar slip

Planar slip

1. **ΔK_{TH} (fatigue threshold)**
2. **Cracks won't initiate below the fatigue threshold**

Twins

Thurston, K. V., Gludovatz, B., Hohenwarter, A., Laplanche, G., George, E. P., & Ritchie, R. O. (2017). Effect of temperature on the fatigue-crack growth behavior of the high-entropy alloy CrMnFeCoNi. Intermetallics, 88, 65-72.

High-strain rate and high-pressure deformation

- 1. Hopkinson bar experiment
- 2. Gas gun impact experiment
- 3. Wave reflection experiment (ultimate tensile strength)
- 4. Shear localization experiment (failure by adiabatic shear bands)
- 5. Ballistic impact

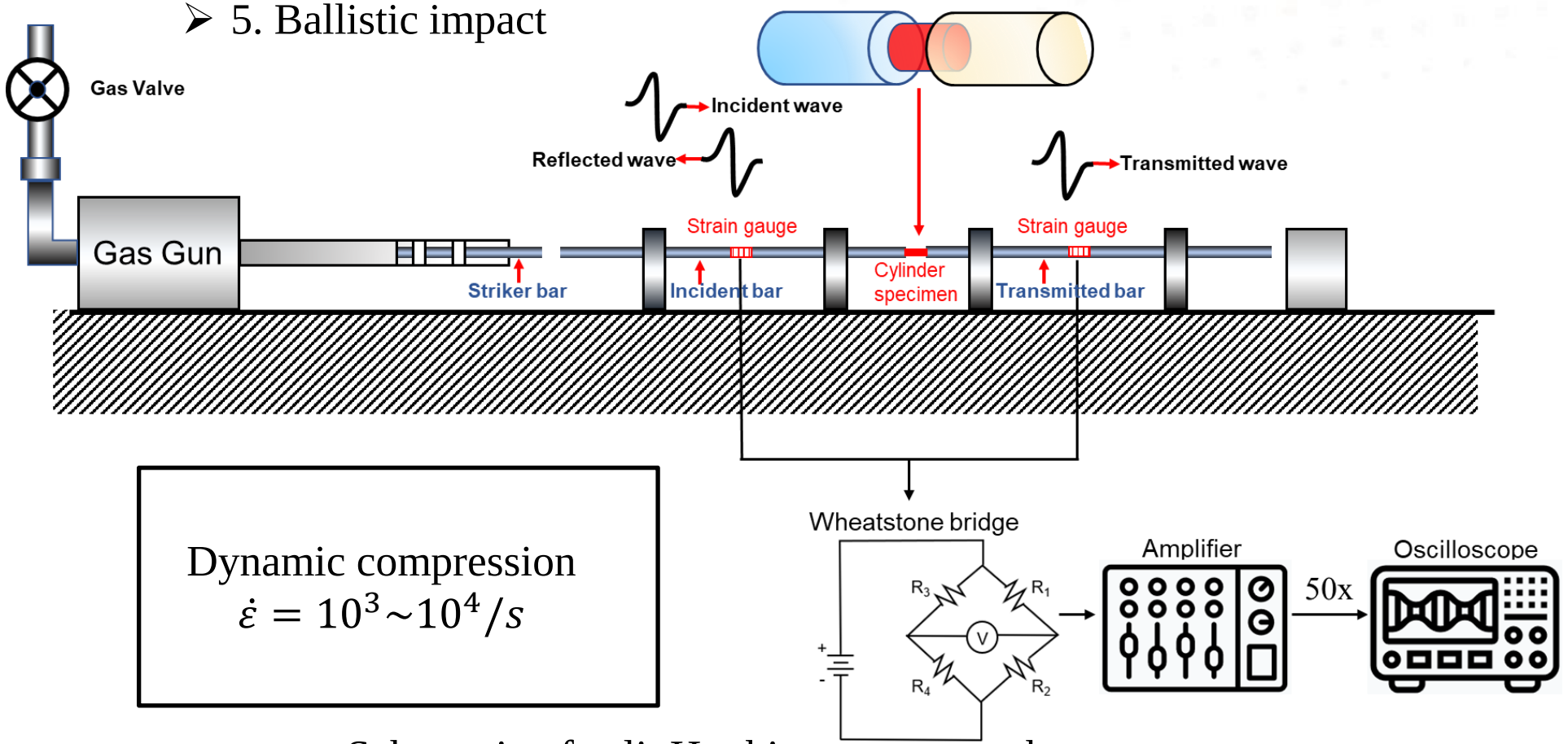

Dynamic compression
$\dot{\varepsilon} = 10^3 \sim 10^4 / s$

Schematic of split Hopkinson pressure bar

Dynamic properties of HEA

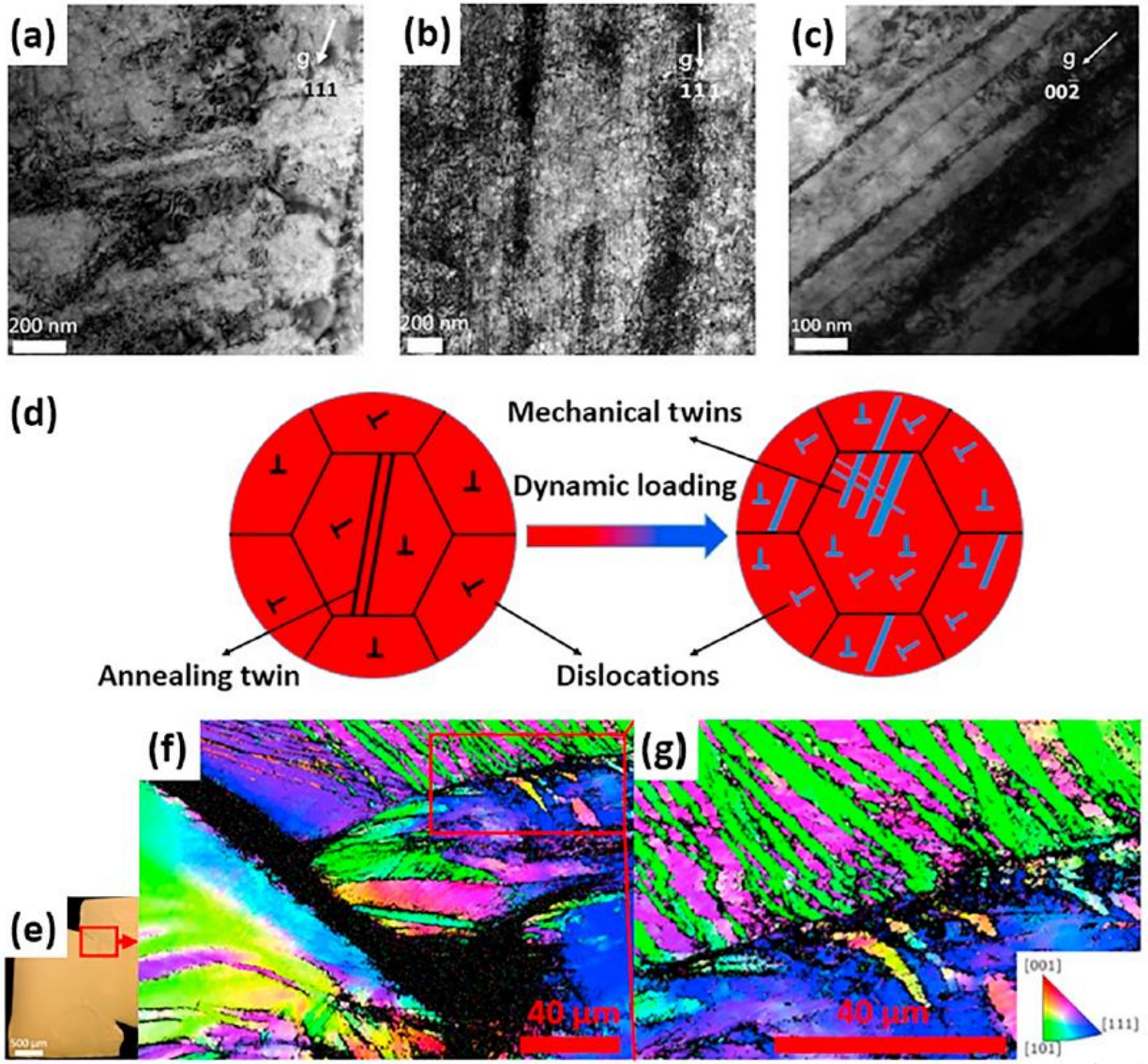

TEM bright-field images of the deformed samples at the strain rates of (a) 10^{-4} s^{-1}; (b) and (c) 1800 s^{-1}.

- Solid solution
- Multiple strengthening effect
  - Forest dislocation
  - Mechanical twinning

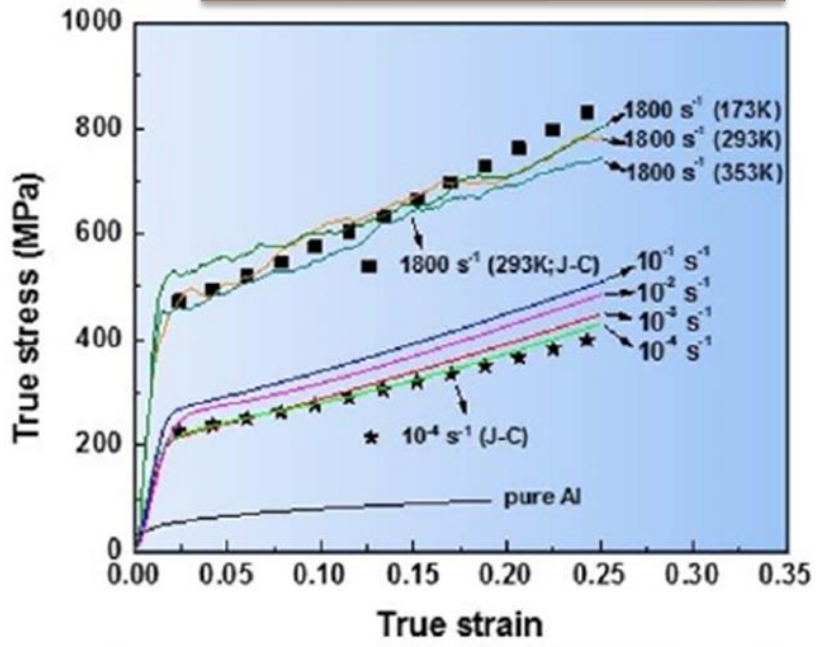

Li Z, Zhao S, Diao H, Liaw P, Meyers M. High-velocity deformation of Al0. 3CoCrFeNi high-entropy alloy: remarkable resistance to shear failure. Scientific Reports 2017;7:42742.

Ballistic performance

Understanding dynamic behavior of HEA at range of 10^3-$10^5 s^{-1}$
(thickness, strength, ductility, toughness, density, projectile parameter, local strains…)

E52100 steel (RC60) projectiles

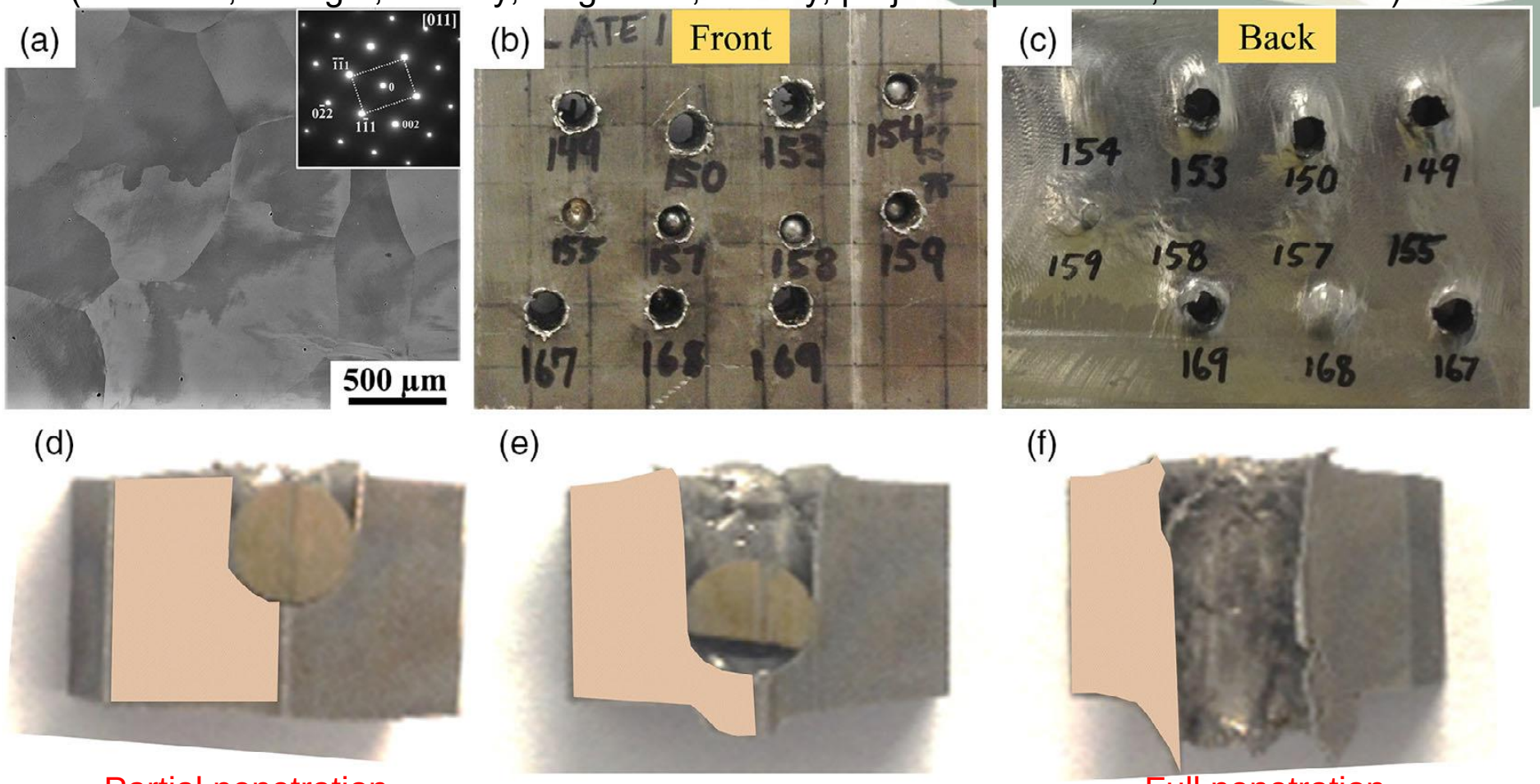

(a) Microstructure of as-cast Al0.1CoCrFeNi HEA (b) front and back side of as-cast HEA plate after ballistic test Penetration at velocity (c) 594m/s (d) 739m/s (f) 994m/s

Muskeri, S., Choudhuri, D., Jannotti, P. A., Schuster, B. E., Lloyd, J. T., Mishra, R. S., & Mukherjee, S. (2020). Ballistic Impact Response of Al0. 1CoCrFeNi High-Entropy Alloy. Advanced Engineering Materials, 2000124.

Ballistic performance

Inner structure (Relatively soft) ← **Crater wall (Hard)**

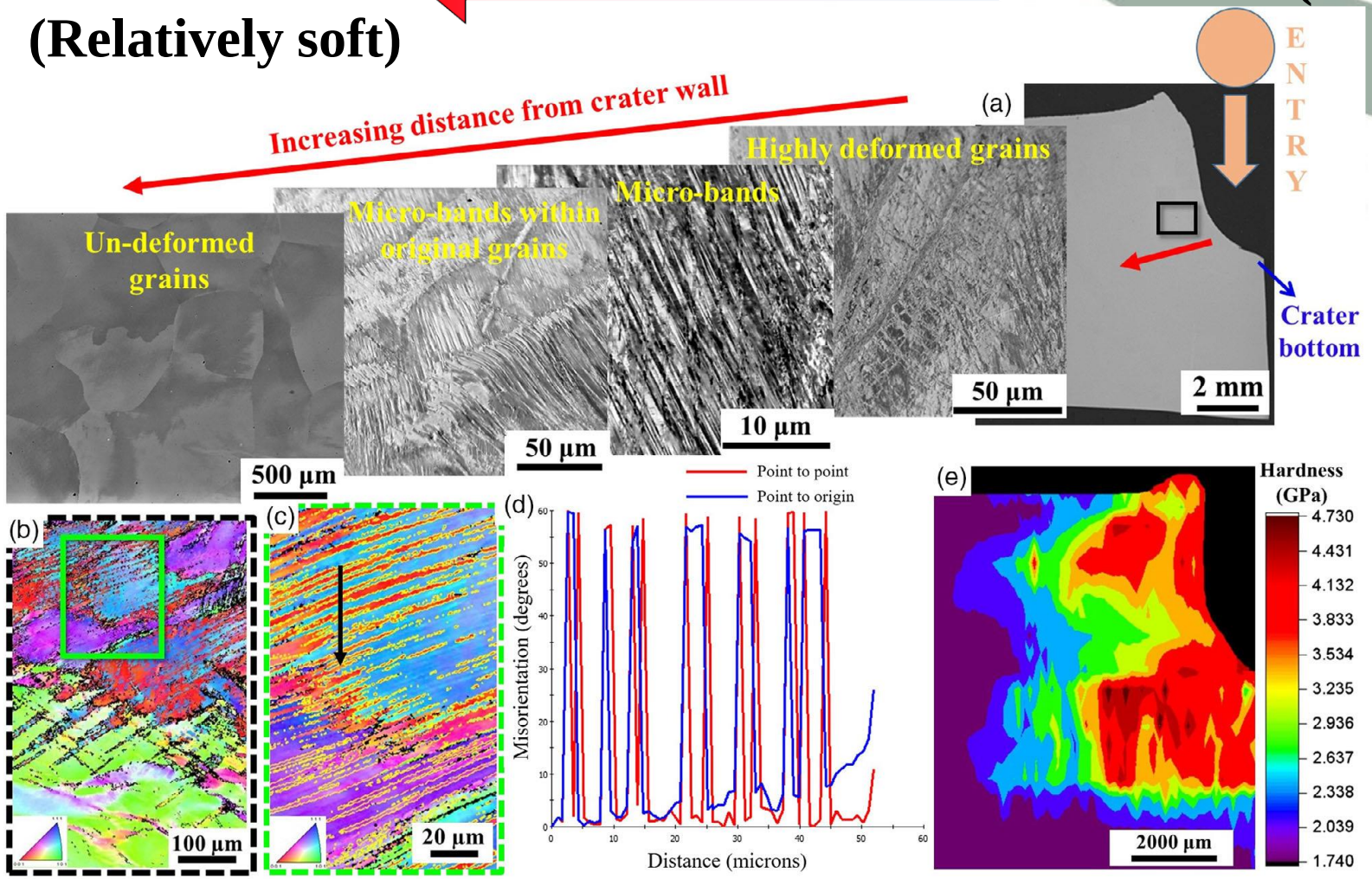

(a)Microstructure as a function of distance from the crater wall (b)(c)IPF map
(d)Misorientation profile (e)nano-indentation hardness contour map

Microband and micro-twinning formation

Due to spherical shock wave on Low SFE metals:

1. Misorientation profile: ~60º(twinning)
2. Misorientation profile: <10º(Microband)

Work hardening

1. No dynamic recrystallization caused by ASB
2. Excellent work-hardening at crater wall

Muskeri, S., Choudhuri, D., Jannotti, P. A., Schuster, B. E., Lloyd, J. T., Mishra, R. S., & Mukherjee, S. (2020). Ballistic Impact Response of Al0. 1CoCrFeNi High-Entropy Alloy. Advanced Engineering Materials, 2000124.

Conclusion

- 1. High thermal stability
- 2. High fracture toughness
- 3. Excellent wear resistance
- 4. Out standing working hardening ability
- 5. Appreciable anti-fatigue and anti-creep ability
- 6. Excellent ballistic impact performance

Future direction

- 1. Light novel high-entropy alloy
- 2. Non-metallic element doped high-entropy alloy
- 3. Wrought processed high-entropy alloy (homogenization, cold rolling/hot rolling)
- 4. BCC-HEA

Challenges

- 1. Formation of different phase
- 2. Identifying useful alloy composition
- 3. Expensive